Palaeogeography, Palaeoclimatology, Palaeoecology 498 (2018) 127–142

Contents lists available at ScienceDirect

Palaeogeography, Palaeoclimatology, Palaeoecology

journal homepage: www.elsevier.com/locate/palaeo

Mid- to late Holocene geomorphological and hydrological changes in the south Taihu area of the Yangtze delta plain, China

Ting Chen[a,b], David B. Ryves[c], Zhanghua Wang[a,*], Jonathan P. Lewis[c], Xuening Yu[a]

[a] State Key Laboratory of Estuarine and Coastal Research, East China Normal University, Shanghai 200062, China
[b] Academy for Advanced Interdisciplinary Studies, Southern University of Science and Technology, Shenzhen 518055, China
[c] Centre for Hydrological and Ecosystem Science, Department of Geography, Loughborough University, Loughborough LE11 3TU, UK

ARTICLE INFO

Keywords:
Coastal wetland
Salinity
Sea level
Freshwater resource
Rice agriculture
Multiproxy analyses

ABSTRACT

The Taihu Plain of the Lower Yangtze valley, China was a centre of rice agriculture during the Neolithic period. Reasons for the rapid development of rice cultivation during this period, however, have not been fully understood for this coastal lowland, which is highly sensitive to sea-level change. To improve understanding of the geomorphological and hydrological context for evolution of prehistoric rice agriculture, two sediment cores (DTX4 and DTX10) in the East Tiaoxi River Plain, south Taihu Plain, were collected, and analysed for radiocarbon dating, diatoms, organic carbon and nitrogen stable isotopes ($\delta^{13}C$ and $\delta^{15}N$), grain size and lithology. These multiproxy analyses revealed that prior to ca. 7500 cal. yr BP, the East Tiaoxi River Plain was a rapidly aggrading high-salinity estuary (the Palaeo-Taihu Estuary). After ca. 7500 cal. yr BP, low salinity conditions prevailed as a result of strong Yangtze freshwater discharge. Subsequently, seawater penetration occurred and saltmarsh developed between ca. 7000 and 6500 cal. yr BP due to accelerated relative sea-level rise. This transgression event influenced a large area of the Taihu Plain during the Holocene, as shown by multiple sediment records from previous studies. Persistent freshwater marsh (or subaerial land) formed due to dramatic shrinkage/closure of the Palaeo-Taihu Estuary after ca. 5600 cal. yr BP when sea level was relatively stable. We speculate that geomorphological and hydrological changes of the East Tiaoxi River Plain played an important role in agricultural development across the Taihu Plain during the Neolithic period. The closure of the Palaeo-Taihu Estuary and the formation of stable freshwater marsh (or subaerial land) after ca. 5600 cal. yr BP were critical preconditions encouraging the rapid rise of rice productivity in the Liangzhu period (5500–4500 cal. yr BP). This development changed the landscape and river systems, and thus provided adequate freshwater supply to the Taihu Plain.

1. Introduction

The lower Yangtze valley, East China is one of the centres where intense rice growth started in the Neolithic period (Zong et al., 2007; Liu and Chen, 2012). Many studies have been focused on the origin and domestication of rice farming in this region during the Neolithic cultural period (Zong et al., 2007; Mo et al., 2011; Liu and Chen, 2012). The first evidence of collection and consumption of wild rice (ca. 9000–10,000 cal. yr BP) was found at Shangshan site, in Zhejiang Province (Liu and Chen, 2012; Zuo et al., 2017). Evidence for rice cultivation also found at the Kuahuqiao site at ca. 7700 cal. yr BP (Zong et al., 2007). Although marine inundation caused by sea-level rise brought rice cultivation to an end at the Kuahuqiao site at ca. 7500 cal. yr BP (Zong et al., 2007), rice farming subsequently expanded to the south of the Hangzhou Bay and in the Taihu Plain, north of Hangzhou Bay (Chen et al., 2008; Zong et al., 2012a; Zheng et al., 2012). Rice domestication started during the period of the Majiabang culture (7000–5800 cal. yr BP), the first Neolithic culture that appeared on the Taihu Plain, though this society still relied mostly on hunting, fishing and gathering (Cao et al., 2006; Fuller et al., 2007; Mo et al., 2011; Zong et al., 2012a; Xu, 2015). More rice cultivation was practiced during the Songze period (5800–5500 cal. yr BP), but hunting, fishing and gathering were still important at that time (Cao et al., 2006; Mo et al., 2011). Subsequently, rice farming intensified and its yield increased dramatically during the Liangzhu culture (5500–4500 cal. yr BP) (Fan, 2011; Mo et al., 2011; Zhuang et al., 2014; Zhang et al., 2015). For example, substantial quantities of carbonised rice were found at several Liangzhu sites (Fan, 2011), one of which even reached to tens of thousands of kilograms; numerous specialised fine stone tools used for rice farming, such as ploughs and sickles, were also found (Mo

* Corresponding author.
E-mail address: zhwang@geo.ecnu.edu.cn (Z. Wang).

https://doi.org/10.1016/j.palaeo.2018.03.012
Received 18 December 2017; Received in revised form 6 March 2018; Accepted 13 March 2018
Available online 20 March 2018
0031-0182/

et al., 2011). Relying on rapid advances in rice farming, the Liangzhu culture developed into a sophisticated and complex society and was considered as one of the most advanced Neolithic societies in the world (Jiang and Liu, 2006; Zhu, 2006; Lawler, 2009; Mo et al., 2011; Zong et al., 2012a; Zhuang et al., 2014).

Several studies suggested that a warm/humid climate promoted the development of rice farming in the lower Yangzte delta (Yu et al., 2000; Chen et al., 2005; Innes et al., 2009, 2014; Patalano et al., 2015), together with ancient people's successful water and landscape management of rice paddies (Zong et al., 2007; Zhuang et al., 2014). Recently, more attention has been paid to the role of the hydrological environment, which is the result of a complex of sea-level, climate and geomorphological conditions (Zong et al., 2007; Qin et al., 2011; Zheng et al., 2012; Long et al., 2014; Patalano et al., 2015). For example, Zong et al. (2007) found that freshwater low-land swamps at the Kuahuqiao site were selected by Neolithic people for rice cultivation. Qin et al. (2011) reported that rice-based agriculture occurred during two intervals of lower salinity, between ca. 7850–7210 cal. yr BP and ca. 3000–2290 cal. yr BP. Although these studies of hydrological background based on individual cores provided insights into our understanding of the development of rice farming in the lower Yangtze valley, new studies on key sites allowing an integrated analysis of previous studies are still required to provide a more detailed environmental context on a regional scale.

We focus here on the hydrological changes during the mid- to late-Holocene in the East Tiaoxi River Plain, part of the southern Taihu Plain (Fig. 1A and B). The East Tiaoxi River Plain is a critical part of the Taihu plain, because it was a palaeo-incised valley during the Last Glacial Maximum (LGM) and was occupied by the Palaeo-Taihu Estuary during the early- to mid-Holocene (Fig. 1C; Hong, 1991). Through this estuary, sea water could have reached the centre of the Taihu Plain, and freshwater from the west uplands, which flows into the Taihu lake at present, instead was discharged into Hangzhou Bay (Hong, 1991). Such hydrologic conditions had restricted the freshwater resource for Neolithic people in the Taihu Plain. Morphological and hydrological changes within the East Tiaoxi River Plain from the Mid-Holocene are therefore potentially critical to understanding the evolution of rice farming in the Taihu Plain over the Neolithic period.

A complete understanding of the evolution of morphological and hydrological environments of the East Tiaoxi River Plain during the mid- to late-Holocene, however, has been hampered by a lack of high-quality sediment archives with reliable dating allowing detailed sedimentological analysis. To address this gap and fulfill the research aim mentioned above, two sediment cores (DTX 4 and DTX10), spanning the last 7100 and 7600 years respectively, were collected beside the Luosheyang Lake and the Qianshanyang Lake in the East Tiaoxi River Plain in 2014 (Fig. 1). Using these two cores, we studied the past morphological and hydrological environments of the East Tiaoxi River Plain over the last 7600 years, by using a multi-proxy approach including lithology, grain size, diatom analysis and organic geochemistry (including stable isotopes of carbon and nitrogen: $\delta^{13}C$, $\delta^{15}N$). Additionally, we compared these new results with the hydrological environment inferred from other parts of the Taihu Plain from previously studied cores (Itzstein-Davey et al., 2007; Atahan et al., 2008; Zong et al., 2011, 2012b; Wang et al., 2012; Innes et al., 2014; Liu et al., 2015). Based on these results, we discuss how changing morphological and hydrological conditions in the East Tiaoxi River Plain influenced the expansion of rice cultivation in the Taihu Plain over the Neolithic period.

2. Study area and site description

During the LGM, the landscape of the Taihu Plain was characterised by a series of river terraces (T1, T2 and T3) and incised valleys (Fig. 1C) cutting through these terraces (Yan and Huang, 1987; Li et al., 2000, 2002; Wang et al., 2012). The terraces T1, T2 and T3 were regions where the thickness of Holocene sediments were at 20–30 m, 5–15 m, and < 5 m, respectively (Yan and Huang, 1987; Li et al., 2000, 2002; Wang et al., 2012). The largest two of these palaeo valleys were the Yangtze valley in the north and the Qiantang valley in the south. The Palaeo-Taihu valley lay along the western highlands, and freshwater discharge from western mountains flowed through it southwards into the Palaeo-Qiantang valley (Yan and Huang, 1987; Hong, 1991; Wang et al., 2012). When sea level rose from −18 m to −4 m between ca. 8600 cal. yr BP and ca. 7300 cal. yr BP, the south part of the Palaeo-Taihu valley became an estuary, allowing sea water from Hangzhou Bay to reach the central Taihu Plain (Hong, 1991; Wang et al., 2012).

Present-day geomorphological and hydrological conditions of the Taihu Plain, however, are dramatically different. Today, the Taihu Plain is characterised by a saucer-like depression, in the centre of which lies Taihu Lake (Fig. 1A), the third largest freshwater lake in China. Taihu Lake receives freshwater inflows (e.g. the East and West Tiaoxi Rivers; Fig. 1A) from the mountainous areas to the west of the Taihu Plain and provides an important freshwater resource for the human population in the Taihu Plain.

The East Tiaoxi River Plain is the southern part of the Taihu Plain and lies between Taihu Lake in the north and the Qiantang River/Hangzhou Bay in the south (Fig. 1A and B). Relief is slightly higher (2–5 m) in the south and east, and lower (< 2 m) in the depression near Taihu Lake. The East Tiaoxi River, the largest river in the East Tiaoxi River Plain, flows northward into Taihu Lake after joining with the West Tiaoxi River in the city of Huzhou.

Luosheyang Lake and Qianshanyang Lake are located near the East Tiaoxi River (Fig. 1B, D and E), and are about 140 km west of Shanghai. They are both naturally open, shallow (< 2 m maximum depth) and flat-bottomed freshwater lakes, through which the East Tiaoxi River and its tributaries flow. Over recent decades, the area of the Luosheyang Lake has been reduced due to extensive marginal development for agriculture (e.g. rice paddies) to about 1.56 km^2, while the Qianshanyang Lake has been almost completely reclaimed.

3. Material and methods

3.1. Coring, sampling, AMS ^{14}C dating and age-depth model

Both cores DTX4 and DTX10, 5.7 and 4.6 m long respectively, were obtained in May 2014 using a gouge corer (Eijkelkamp Company, the Netherlands), with a diameter of 3 cm. Core DTX4 (30°38′16.465″ N, 120°05′28.546″ E) was collected from a reclaimed agricultural field which was previously the edge of the Luosheyang Lake, and core DTX10 from a rice paddy near present Qianshanyang Lake (Fig. 1B, D and E). Lithology of both cores was examined carefully during the drilling, including particle composition, structure, colour, and presence of plant macrofossils. Recent cultural sediments at the top of each core were removed (the uppermost 80 cm at DTX4 and 20 cm at DTX10). Ten plant macrofossils (excluding root material) and organic-rich samples from the two cores were dated via AMS ^{14}C dating by Beta Analytic, USA (Table 1). All conventional dates were calibrated using the INTCAL 13 database (Reimer et al., 2009) and software Calib 7.1 (Stuiver et al., 2015) and calibrated dates with two sigma were presented as 'medial point ages ± standard deviation' (Table 1). A linear interpolation method was used to construct the age-depth model, using the program "Clam" with 10,000 iterations (Blaauw, 2010; Fig. 2). The sedimentation rate (SR), the best estimated age and the minima and maxima of age confidence intervals were calculated every 2 cm (core DTX4) and 4 cm (DTX10) simultaneously, using the "Clam" program. In addition, a sedimentation hiatus was identified in core DTX10 at a sediment depth of 1.0 m due to a leaching structure indicative of pedogenesis (0.88–1.0 m).

Sediment subsamples were selected at 2 to 10 cm intervals, using 2 to 5 cm thick slices, with thickness chosen according to sedimentation rate: in core DTX4, every 4 cm interval (4 cm thick) from 0.8–1.2 m,

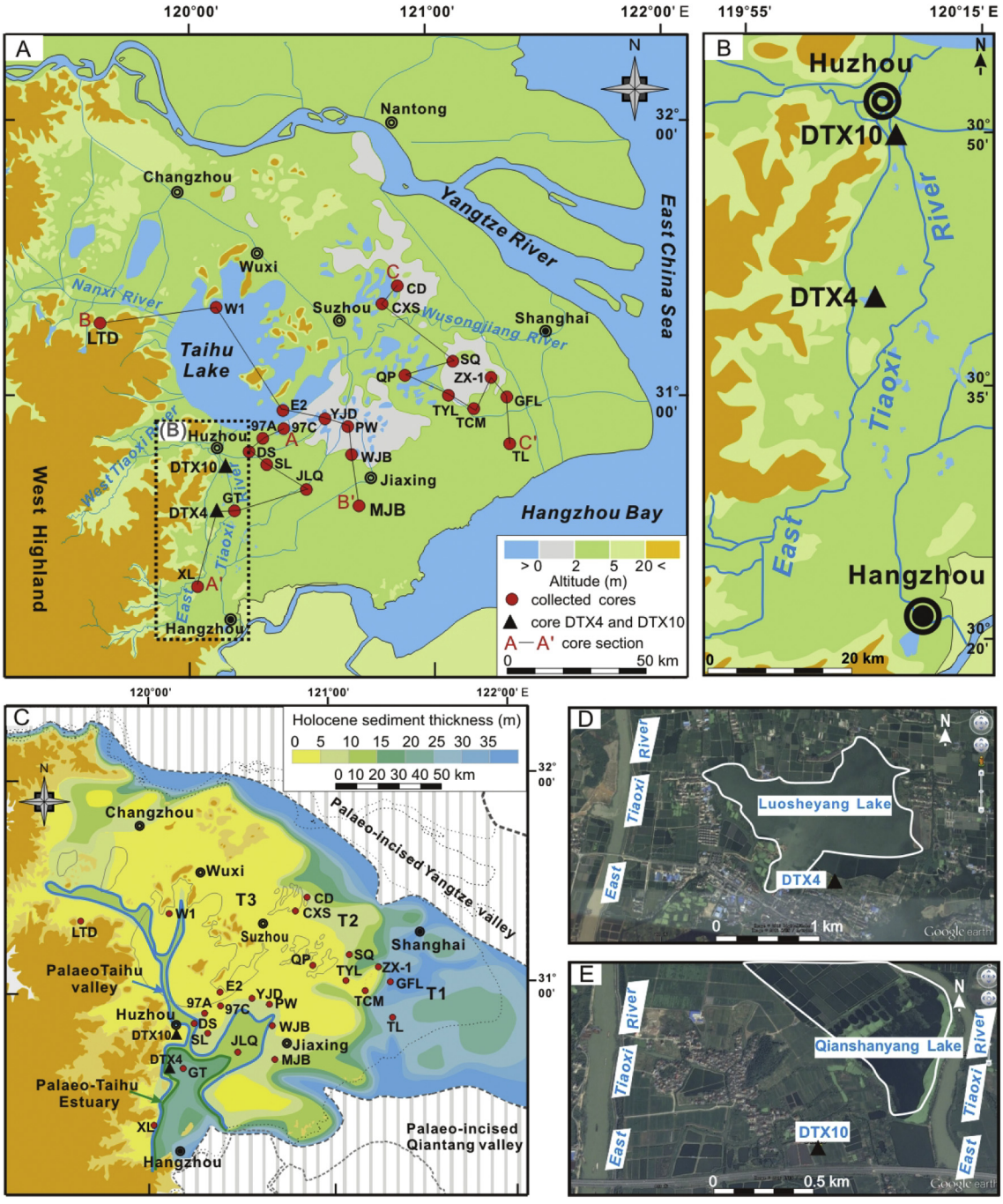

Fig. 1. Maps of the Taihu Plain and location of study sites. (A) Map of the present Taihu Plain (after Song et al., 2013), showing geomorphology, hydrology and locations of cores DTX4 and DTX10, and cores collected from previous studies (red solid circles; references in Supplementary Table 1). (B) Map of the East Tiaoxi River Plain, including West and East Tiaoxi River and locations of cores DTX4 and DTX10. (C) Palaeotopographical map of the Taihu Plain during the Last Glacial Maximum (after Wang et al., 2012), showing the Palaeo-Taihu valley (blue solid line) and Palaeo-Taihu Estuary (green solid line). (D) and (E) Remote sensing image in 2016, around Luosheyang Lake and Qianshanyang Lake from Google Earth, showing part of East Tiaoxi River and locations of cores DTX4 and DTX10, respectively. (For interpretation of the references to colour in this figure legend, the reader is referred to the web version of this article.)

5 cm (5 cm thick) from 1.2–1.8 m, 2 cm (2 cm thick) from 1.8–2.14 m, 3 cm (3 cm thick) from 2.14–2.5 m, and 10 cm (5 cm thick) from 2.5–5.7 m; in core DTX10, every 4 cm (4 cm thick) from 0.2–2.3 m, and 10 cm (5 cm thick) from 2.3–4.6 m. A total of 84 and 77 subsamples were obtained for core DTX4 and DTX10 respectively. All subsamples were stored in a fridge at 4 °C prior to analyses.

3.2. Diatom analysis

Diatom concentrations were low in most samples, with a total of only 29 samples in core DTX4 and 10 in core DTX10 containing diatoms at high enough concentration to permit using the standard water bath method (Renberg, 1990; Battarbee et al., 2001). Due to extremely low diatom concentrations, 8 samples in core DTX4 and 19 in core DTX10, were treated with heavy liquid separation (sodium polytungstate, SPT) using the following procedures (Battarbee and Kneen, 1982; Battarbee et al., 2001). After organic matter and carbonate were removed using hydrogen peroxide (H_2O_2) and HCl, clay grains were removed by adding a few drops of weak NH_3 solution (Battarbee et al., 2001). Then, the non-toxic heavy liquid SPT ($3Na_2WO_4 9WO_3 \cdot H_2O$) with a density of

Table 1
AMS ^{14}C dating results of core DTX4 and DTX10.

Core name	Depth (m)	Dated material	δ^{13}C (‰)	Conventional age (yr BP)	Calibrated age (2 sigma, cal. yr BP)	Median Calibrated age (cal. yr BP)	Lab. code
Core DTX4	1.21	Plant fragments	−27.2	1610 ± 30	1560–1410	1485 ± 75	Beta-383485
	1.45	Plant fragments	−28.8	940 ± 30	930–785	858 ± 73	Beta-406458
	1.81	Plant fragments	−27.8	2860 ± 30	3065–2920	2993 ± 73	Beta-383486
	1.91	Plant fragments	−26.4	4680 ± 30	5575–5550	5562 ± 13	Beta-406459
	2.5	Organic-rich mud	−25.7	5680 ± 30	6500–6405	6453 ± 48	Beta-382369
	5.33	Plant fragments	NA	6150 ± 30	7160–6950	7055 ± 105	Beta-383487
Core DTX10	0.88	Plant fragments	NA	2720 ± 30	2870–2760	2815 ± 55	Beta-382371
	2.3	Plant fragments	−27.6	6650 ± 30	7580–7480	7530 ± 50	Beta-382366
	2.91	Organic-rich mud	−25.1	8380 ± 30	9475–9400	9438 ± 38	Beta-385582
	4.25	Plant fragments	−26.1	6780 ± 40	7680–7575	7628 ± 53	Beta-385583

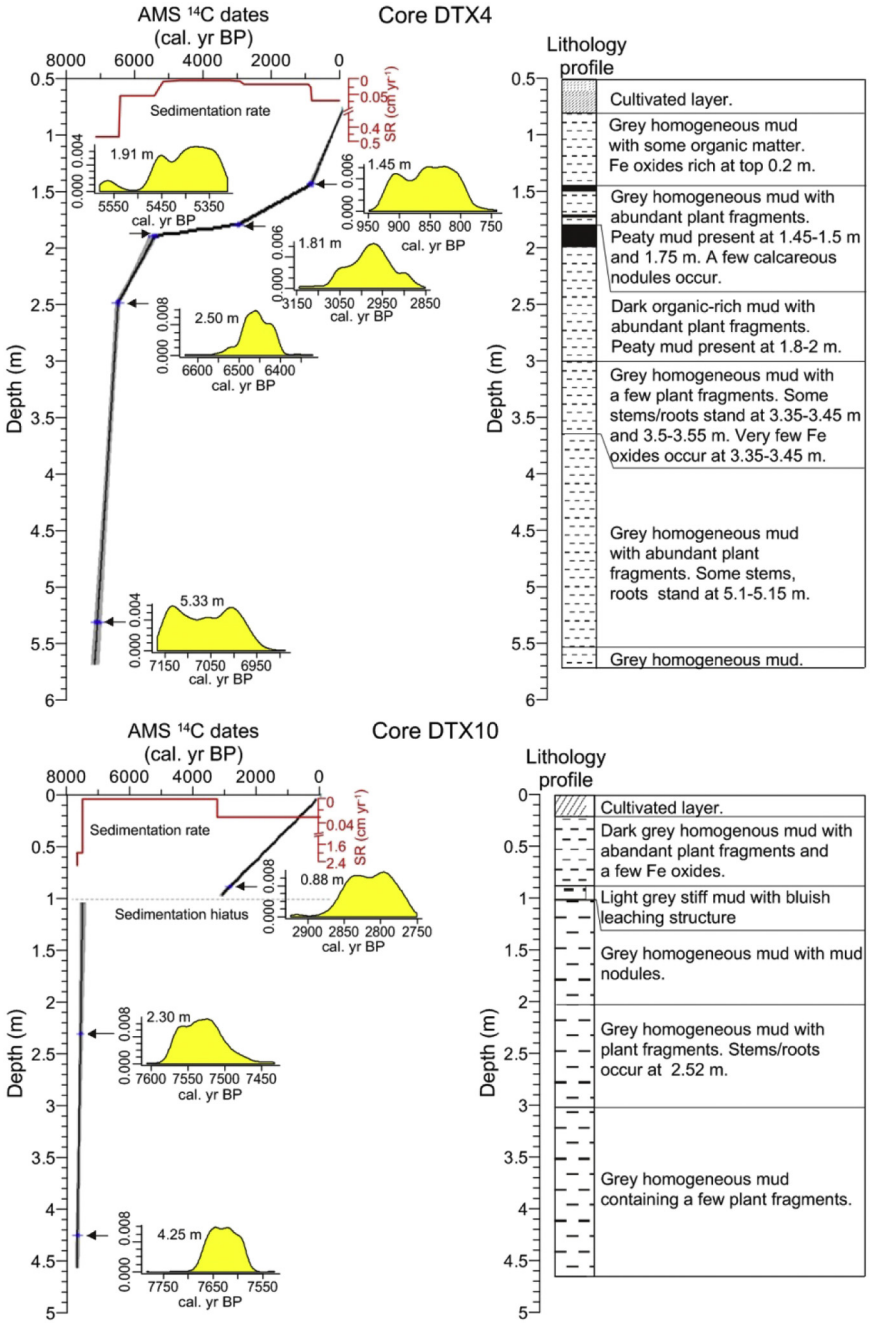

Fig. 2. Age-depth model, sedimentation rate (SR) and density distribution of AMS ^{14}C dates (shaded in yellow) basing on the "Clam" program (Blaauw, 2010), and lithology profile for core DTX4 and DTX10. A sedimentation hiatus was identified at 1.0 m in core DTX10 because of clear indications of pedogenesis (leaching) apparent in the lithology between 0.88 and 1.0 m. (For interpretation of the references to colour in this figure legend, the reader is referred to the web version of this article.)

2.26 g ml^{-1} was used twice to separate diatoms from mineral grains with a density above this. Diatom slides were made in the regular way using the diatom-enriched supernatant taken from the top of SPT solutions, after washing with distilled water. A known number of microspheres were added to all samples to assess diatom concentration (Battarbee and Kneen, 1982). The average number of diatoms counted for samples prepared with regular water-bath and SPT method is 266 and 269 valves, respectively, in core DTX4, with the exception of one sample at 5.675 m, for which only 111 valves were counted due to extremely low diatom concentration. The number of diatoms counted for regularly treated samples was lower in core DTX10 than that in core DTX4 due to lower diatom concentration, but counts of at least 174 valves were obtained with an average of 192, while for SPT treated samples, over 270 valves with an average of 331 were counted. Valves were identified to species level where possible using general (Krammer and Lange-Bertalot, 1986, 1988, 1991a, 1991b; http://westerndiatoms.colorado.edu/) and more specialised coastal floras (Witkowski et al., 2000). Diatoms were also classified into their salinity (freshwater, brackish and marine) and habitat preferences (planktonic, benthic), based on the literature and website resources (e.g. van der Werff and Huls, 1976; Vos and de Wolf, 1993; Ryves et al., 2004; http://craticula.ncl.ac.uk/Molten/jsp/; http://www.marinespecies.org/) and ecological knowledge.

In most samples some signs of diatom dissolution were apparent: e.g. thinner valve walls in the sub-fossil material. Therefore, the state of dissolution for each valve was recorded and the F-index, the ratio of pristine valves to the sum of pristine and dissolved valves, was calculated for each sample (Ryves et al., 2001). Even where the standard water-bath method was suitable, and diatom concentrations were higher (generally in the fresh water phases), preservation was judged not consistently good enough to support applying a salinity model (which remain robust; Juggins, 2013), as poor preservation is known to cause bias in model outputs (e.g. Ryves et al., 2006, 2009). Percentage abundances of diatom data were calculated and plotted using the stratigraphic software package C2 (Juggins, 1991–2009). Diatom zones were determined based on cluster analysis using the CONISS function in the program Tilia 2.0.41.

3.3. Grain size analysis

Grain size analyses were conducted on each subsample. These samples were firstly pretreated with 10% H_2O_2 and then 10% HCl to remove organic matter and carbonates respectively, and then washed in distilled water to remove residual HCl. Following this, 5 ml of 5% Calgon® (sodium hexametaphosphate) was added to each sample before shaking in an ultrasonic bath for 15 min to prevent flocculation of fine-grained particles (Beuselinck et al., 1998). Measurements were performed with a Beckman Coulter Laser Diffraction Particle Size Analyzer (LS13320).

3.4. Measurement of carbon and nitrogen element and their stable isotopes

Samples for total organic carbon (TOC), total nitrogen (TN), $\delta^{13}C$ and $\delta^{15}N$ analysis were firstly freeze-dried, milled and sieved with a 74 μm (200 mesh) sieve. The fine fraction was collected and a subsample treated with 1 M HCl to remove carbonate followed by washing for four to five times with distilled water before drying in an oven at 45 °C. Samples without additional treatment of HCl were used to measure TC and TN, while carbonate-free samples were analysed for TOC and isotopic carbon and nitrogen (Zhang et al., 2007).

TC, TOC and TN were measured using an organic element analyzer (Carlo-Erba model EA1110, Italy) in the State Key Laboratory of Marine Geology at Tongji University, China. TOC concentration was calibrated with Eq. (1) (Yang et al., 2011):

$$TOC\,(\%) = TOC_{measured}\,(\%) \times (12 - TC\,(\%))/(12 - TOC_{measured}\,(\%)) \quad (1)$$

TOC/TN refers to the weight ratio of TOC (%) to TN (%) in this paper. Stable isotopic carbon and nitrogen were measured using a Thermo Deltaplus XL mass spectrometer (continuous flow mode) at the Third Institute of Oceanography, State Oceanic Administration, China. The stable isotopic ratios were expressed as $\delta^{13}C$ and $\delta^{15}N$, in standard units per mil (‰), with respect to PeeDee Belemnite (PDB) and atmospheric nitrogen, respectively. The standard samples used for carbon and nitrogen isotope measuring referred to Urea#2 and Acetanilide#1 from Biogeochemistry Laboratories Indiana University. The precision for $\delta^{13}C$ and $\delta^{15}N$ were < 0.2‰ and < 0.3‰, respectively, based on replicated measurements (n = 5).

TOC/TN ratio and their isotopes are widely used to trace the source of organic matter in lakes and river-estuary-marine systems (Müller and Mathesius, 1999; Meyers, 2003; Wilson et al., 2005; Lamb et al., 2007; Leng and Lewis, 2017). Previous studies have found that TOC/TN ratios are > 12, 4–6, and < 10 for terrestrial vegetation, bacteria, and algae respectively (in Müller and Mathesius, 1999; Lamb et al., 2007; Leng and Lewis, 2017 and references). $\delta^{13}C$ values are in a range of −21 to −31‰, −20 to −30‰, −17 to −22‰ for typical terrestrial C_3 plants, freshwater plankton, and marine plankton respectively (Müller and Voss, 1999 and references in; Lamb et al., 2007; Leng and Lewis, 2017 and references in). Terrestrial plants usually have relative low $\delta^{15}N$ values compared with aquatic plankton (Thornton and McManus, 1994; Middelburg and Nieuwenhuize, 1998; Müller and Voss, 1999). These values are the underlying principles on which we base our interpretation of TOC/TN, $\delta^{13}C$ and $\delta^{15}N$ profiles in cores DTX4 and DTX10.

3.5. Collection of previous archive cores and palaeogeographic reconstruction of the Taihu Plain

To correlate morphological and hydrological conditions in the East Tiaoxi River Plain to other parts of the Taihu Plain and reconstruct palaeohydrological conditions of the whole Taihu Plain, previously published borehole records were compiled, selecting only those which have good chronological (radiocarbon age) control. In total, 23 sediment cores were selected and subdivided into 3 sections A-A′, B-B′ and C-C′ (Fig. 1A and C) to make stratigraphic comparisons (core details including location, dating depth, dating material, dating results and references are provided in Supplementary Table 1). Conventional ages in these cores were calibrated in software Calib 7.1 (Stuiver et al., 2015) using the INTCAL 13 database where dating materials were plant fragments, organic rich mud, seeds, wood and pollen residues, and the Marine 13 database and ΔR value of 135 ± 42 when dating materials were marine molluscs (Yoneda et al., 2007). A linear interpolation method was used to construct ages for key depths, based on the program “Clam” with 10,000 iterations (Blaauw, 2010).

Using sedimentary, morphological and hydrological changes obtained in our new cores (DTX10 and DTX4 presented here) together with those inferred in the 23 selected existing cores, stratigraphic transections for the sections A-A′ B-B′ and C-C′ were reconstructed. Accordingly, sedimentary morphological and hydrological conditions across the whole Taihu Plain were reconstructed for several periods between ca. 7500 and ca. 5500 cal. yr BP, associated with palaeotopography contexts during the LGM (Fig. 1C; Hong, 1991; Li et al., 2002; Wang et al., 2012) and relative sea-level changes in the Yangtze delta during the Holocene (Zong, 2004; Wang et al., 2012, 2013).

4. Results and interpretation

4.1. Lithology, AMS ^{14}C dating and sedimentary accumulation rates in cores DTX4 and DTX10

4.1.1. Core DTX4

The bottom 2.7 m of the sequence (i.e. 5.7–3.0 m depth) consisted of grey homogeneous mud with abundant plant fragments (Fig. 2). This changed to dark, organic-rich mud over 3.0–2.0 m, followed by a peaty mud layer (2.0–1.8 m). Grey homogeneous mud with abundant plant fragments reoccurred at 1.8–1.45 m, with peaty mud at 1.75 and 1.5–1.45 m. Plant fragments declined from 1.45 m to the top. In total, six AMS ^{14}C dates were obtained over the sequence (Table 1). These ages are in reasonable sequential order with the exception of the date obtained at 1.21 m, which is older than the age obtained from the peaty mud at 1.45 m. We reject this reversed age because it could be derived from reworked plant macrofossils. By contrast, the age from peaty mud is more reliable because the peaty mud was formed by in situ deposition of local marsh plants. Stanley (2000) reported that it is quite common that radiocarbon dates of Holocene sediments do not become progressively older with depth in cores from the Yangtze delta, due to the introduction of old carbon during sediment transport and storage. This "old carbon" phenomenon has also been discussed by Wang et al. (2012). The remaining five dates were used to generate the linear interpolation age-depth model and to calculate sedimentation rate (SR) with the program "Clam" (Blaauw, 2010; Fig. 2). Relatively high SR of 0.47 cm per year (cm yr^{-1}) from 7050 to 6450 cal. yr BP (5.33–2.5 m) was followed by a reduced SR of 0.056 cm yr^{-1} from 6450 to 5560 cal. yr BP (2.5–1.91 m) and 0.004 cm yr^{-1} from 5560 to 2990 cal. yr BP (1.91–1.81 m). After 2990 cal. yr BP, SR increased to 0.017 from 1.81–1.45 m and to 0.072 from 1.45–0.8 m (Fig. 2).

4.1.2. Core DTX10

From the base of the sequence (4.7 m) to 1.0 m, lithology was grey homogeneous mud with plant fragments occurring occasionally (Fig. 2). This changed to light grey homogeneous, stiff mud with bluish leaching structures at 1.0–0.88 m, indicating subaerial pedogenesis processes and hence a sedimentation hiatus. At 0.88 m, it became dark, homogeneous mud with abundant plant fragments to the top. Four AMS ^{14}C dates were obtained throughout the sequence (Table 1). The reversed date at 2.91 m (9475–9400 cal. yr BP) was rejected, as we argue that it was also derived from reworked plant material as discussed earlier (Stanley, 2000; Wang et al., 2012). The remaining three dates were used to construct the age-depth model and to calculate SR based on "Clam" (Fig. 2). When running the age-depth model in "Clam", a sedimentation hiatus was set at 1.0 m, as reflected by the pedogenesis at 1.0–0.88 m. Core DTX10 showed similar SR pattern to core DTX4. Before 7460 cal. yr BP (below 1 m), SR was high (up to 2 cm yr^{-1}), thereafter pedogenesis and a sedimentation hiatus occurred from 7460 to 2810 cal. yr BP (1.0–0.88 m). Following this, SR rose to 0.03 cm yr^{-1} after 2810 cal. yr BP (0.88–0 m).

4.2. Diatom assemblages

4.2.1. Core DTX4

A total of 236 species were identified and four habitat groups were distinguished including freshwater, salt-tolerant freshwater, brackish and marine species. No diatoms were found from 2.0–2.75 m and 1.2–1.45 m. All diatom species > 5% were plotted as percentages of the total assemblage in Fig. 3.

In Zone I (5.7–5.0 m, 7140–6990 cal. yr BP), diatom concentration was the highest over the whole sequence (avg. 6.84 × 10^3 valve g^{-1} wet weight). On the contrary, F-index was the highest, with 29.1% of valves on average remaining in pristine state (Fig. 3). The two most abundant species were *Aulacoseira granulata* (avg. 13.8%) and *Aulacoseira ambigua* (avg. 12.6%). These two salt-tolerant freshwater planktonic species with low salt tolerance favour shallow fresh water (low salinity tolerant) and well-mixed hydrological conditions (Kilham, 1990; Owen and Crossley, 1992). Freshwater benthic species such as *Pseudostaurosira brevistriata* (avg. 9.2%), *Staurosira construens* (avg. 4.9%) and its varieties of *Staurosira construens f. venter* (avg. 4.3%) and *Staurosira construens f. construens* (avg. 2.5%) followed. Brackish benthic (e.g. *Diploneis smithii* var. *dilatata*, *Amphora copulata*) and freshwater benthic species (e.g. *Gomphonema gracile/parvulum*, *Eunotia minor*) were also found, but at low percentages (< 3% for each). The average percentage of freshwater species (including both freshwater and freshwater with low salt tolerance groups) in this section was 88.5% while brackish species accounted for only 9.9%, and the average percentage of planktonic species was 39.5%.

In Zone II (5.0–4.0 m, 6990–6780 cal. yr BP), the diatom concentration decreased to 3.23 × 10^3 valve g^{-1} wet weight, while the F-index declined slightly to 13.9%. Relative concentration of freshwater planktonic (e.g. *A. ambigua*) and freshwater benthic with low salt tolerance species (e.g. *P. brevistriata*, *S. construens* and its varieties of *S. construens f. venter* and *S. construens f. construens*) decreased slightly, with the exception of *A. granulata* which remained fairly constant. Correspondingly, percentages of brackish and freshwater benthic species (including *D. smithii* var. *dilatata*, *A. copulata*, *Gyrosigma acuminatum*, *G. gracile*) rose slightly. A brief recovery of the low salinity planktonic (*A. ambigua/granulata*) and benthic (*P. brevistriata*, *S. construens* and its varieties) group occurred at the top of this unit (4.0–4.4 m). The average percentages of freshwater species dropped to 78.5% while brackish species rose to 19.3%, and planktonic species decreased to 29.5%.

In Zone III (4.0–2.7 m, 6780–6500 cal. yr BP), a further drop of diatom concentration (avg. 2.23 × 10^3 valve g^{-1} wet weight) occurred, accompanied by increasing dissolution (F-index dropped to 7.9%). *A. granulata* remained relatively abundant (avg. 10.8%), despite a further decrease in the low salinity assemblages, giving way to brackish benthic (e.g., *D. smithii* var. *dilatata*, *A. copulata*, *Gyrosigma strigilis* and *Navicula menisculus*) and freshwater benthic (e.g. *G. accuminatum*, *G. gracile*, *Cymbella tumida*) species. The average percentage of freshwater species declined to 66.7% and brackish species rose to 31.6%, with the planktonic group falling to 20.4%.

A remarkable shift in the diatom assemblage occurred in Zone IV (2.0 m from the top, 5570 cal. yr BP to the present), associated with a slight increase in diatom concentration (avg. 2.85 × 10^3 valve g^{-1} wet weight) and increase in F-index (avg. 9.7%). This unit was dominated by freshwater benthic and epiphytic species of *G. parvulum/gracile*, *E. minor*, *Fragilaria vaucheriae* and *Cymbella silesiaca*, with very few brackish benthic (e.g. *D. smithii* var. *dilatata*, *A. copulata*, *N. menisculus*, *G. strigilis*) and freshwater to low salinity tolerant planktonic species (e.g. *A. granulata/ambigua*). In the uppermost samples (1.1–1.0 m), *Diadesmis confervacea* became frequent (up to 45%), an indicator of aerial/terrestrial or very shallow-water conditions (Gell et al., 2007). Freshwater species accounted for 95.1% and brackish species were < 5% on average, while planktonic species accounted for only 3.9% of the assemblage.

4.2.2. Core DTX10

Diatom concentration was low with an average value of 0.46 × 10^3 valve g^{-1} wet weight for the whole core (Fig. 4), probably resulting from strong dissolution of diatoms reflected by low average F-index value (~7.4%) and dilution caused by high sediment accumulation rates or low diatom productivity. No diatoms were found from 2.7–3.0 m and 0.84–2.0 m and only a few broken diatom fragments were found on slides for samples from the top to 0.84 m. Preservation in one sample at 0.66 m was slightly better, but most remaining diatoms were the dissolved centres of large benthic genera *Pinnularia* or *Cymbella*, but which cannot be identified to species level. For other samples from 0.3 to 0.84 m, broken fragments of freshwater genera, such as *Eunotia* species, were seen. A total of 154 species were identified for the

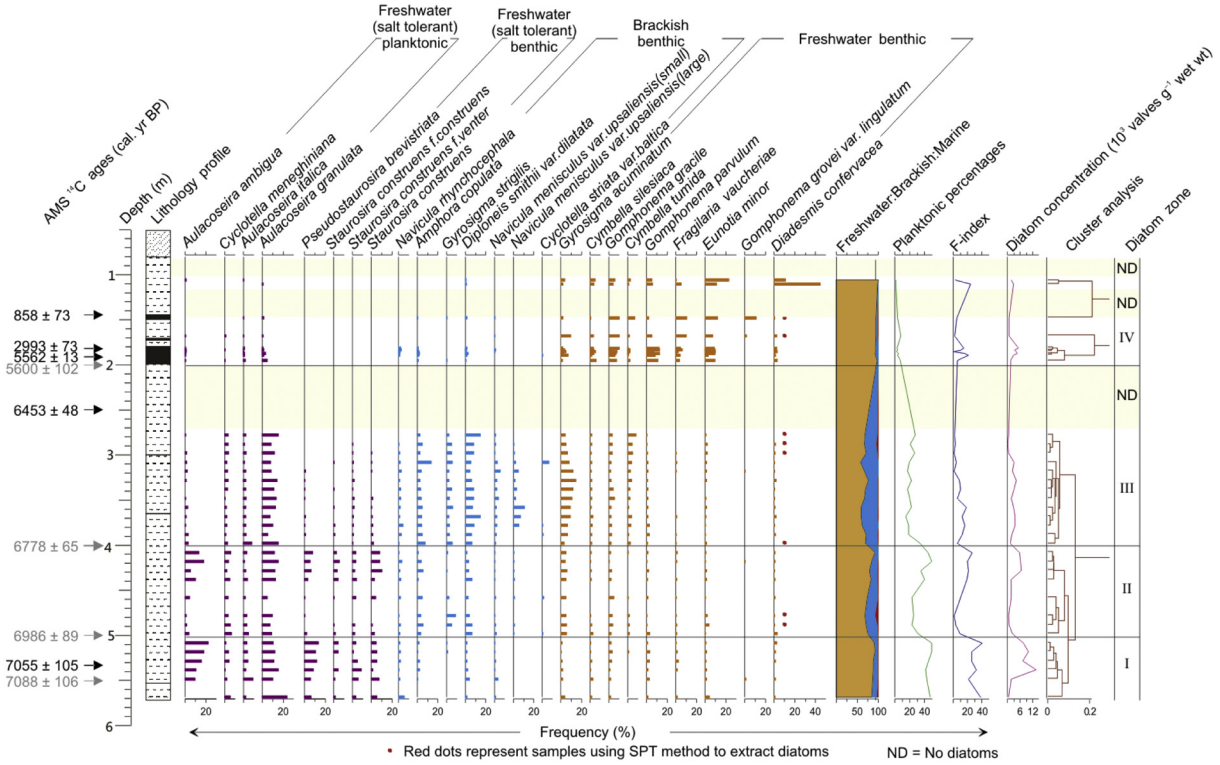

Fig. 3. Diatom taxa in core DTX4 (> 5% relative abundance) separated into freshwater (including both freshwater and salt-tolerant freshwater groups), brackish, and marine species, percentages of planktonic species, F-index and diatom concentration. Calibrated AMS ^{14}C dates (in dark) and calculated age regions (in grey) for important boundaries are presented as 'medial point ages ± standard deviation', as in Figs. 4, 5 and 7.

whole sequence and diatom species > 5% plotted as relative abundance in Fig. 4.

The diatom assemblage from the base to 2.0 m (7650–7520 cal. yr BP; except 2.7–3.0 m where no diatoms were found) was dominated by *Cyclotella striata* (avg. 22.5%), which is usually abundant in river-mouth/estuarine environments (Ryu et al., 2005), *Actinoptychus senarius* (avg. 19.8%), the relatively low-salinity coastal planktonic species (Grönlund, 1993; Hasle and Syvertsen, 1996), *Paralia sulcata* (avg. 9.3%) which is used as a marker for the coastal East China Sea (Tada et al., 1999; Ryu et al., 2005), and *Chaetoceros* spp. resting spores, typical marine species (avg. 9.2%). Other species found but in relatively low percentage were coastal species of *Thalassiosira nanolineata* (Grönlund, 1993; Hasle and Syvertsen, 1996) and brackish benthic species such as *Diploneis smithii* var. *dilatata/smithii, Nitzschia granulata, Cocconeis costata* var. *pacifica*. In total, percentages of marine and brackish species were 56.3% and 37.9% on average respectively, and planktonic species 77.4% (including tychoplanktonic taxa).

Although preservation was very poor in samples from the top to 0.84 m, it was clear that the original diatom assemblage was completely different. Almost 99% of diatom valves (as represented by the sample at 0.66 m) belonged to freshwater benthic species (including *Gomphonema gracile*, *Cymbella aspera*, *Eunotia minor*, *E. formica* and unidentified *Pinnularia* and *Cymbella* species). We argue that the switch from a brackish/marine to a freshwater assemblage from Zone I to Zone II reflects a real change to the salinity and hydrology of the system as the vestigial fragments of diatoms in Zone II are resistant and have distinctive morphologies. Had these taxa been part of the assemblage of earlier sections, they would have been significant aspects of the assemblages there also. By the same token, most of the taxa in the earlier, more marine parts of Zone I are also very resistant to dissolution (e.g. *Chaetoceros* cysts, *Paralia sulcata*, *Cyclotella striata*) with distinctive taphonomic end-members, and would have appeared in Zone I had they been present in the original assemblage in that section. Thus we are confident that Zone I was deposited under brackish-marine conditions while Zone II represents a freshwater system.

4.3. Grain size, TOC/TN ratio and C-N stable isotopes

Based on grain size composition, TOC, TN, TOC/TN and C-N stable isotope (δ^{13}C, δ^{15}N) variations, cores DTX4 and DTX10 were divided into five and three zones, denoted as Zone I–V, respectively (Figs. 5–7). Zone II and V in core DTX4 (Fig. 5) were both divided into three sub-zones based on variation of TOC/TN ratio, δ^{13}C and δ^{15}N values. Zone I and III in core DTX10 were also divided into three and two sub-zones respectively.

4.3.1. Core DTX4

In Zone I (5.7–5.5 m, 7140–7100 cal. yr BP), clay content (< 4 μm) was around 24.8%, silt (4–63 μm) 67.7%, and sand (63–2000 μm) 7.3% on average. In Zone II (5.5–2.5 m, 7100–6450 cal. yr BP), clay content (avg. 19.6%) decreased and silt content (avg. 72.7%) increased slightly, particularly for grains between 16 and 63 μm. No change occurred in sand content. Particles between 8 and 16 μm increased slightly while particles between 16 and 63 μm fell in II_3 (4.0–2.5 m, 6780–6450 cal. yr BP) compared to II_1 (5.5–5.0 m, 7100–6990 cal. yr BP) and II_2 (5.0–4.0 m, 6990–6780 cal. yr BP). Grain size assemblages in Zone III (2.5–2.0 m, 6450–5570 cal. yr BP) remained similar to those of Zone II, followed by a sudden increase in sand content in Zone IV (2.0–1.8 m, 5570–2990 cal. yr BP) and clay content in Zone V (1.8 m to the top, 2990 cal. yr BP to the present) with an opposite trend in silt content.

The linear correlation of TOC to TN (Fig. 6A) implied that TN content was controlled mostly by organic matter, while the positive TN intercept of 0.07% indicated a slight contribution from inorganic nitrogen. Plots of δ^{13}C and δ^{15}N against TOC/TN revealed a mixture of freshwater and marine algae and terrestrial C_3 plants (Fig. 6B and C). In Zone I, TOC (avg. 0.47%), TN (avg. 0.06%) and TOC/TN (avg. 7.48) minima coincided with relatively high δ^{13}C (avg. −24.04‰) and δ^{15}N (avg. +3.16‰), indicating contribution from marine plankton and

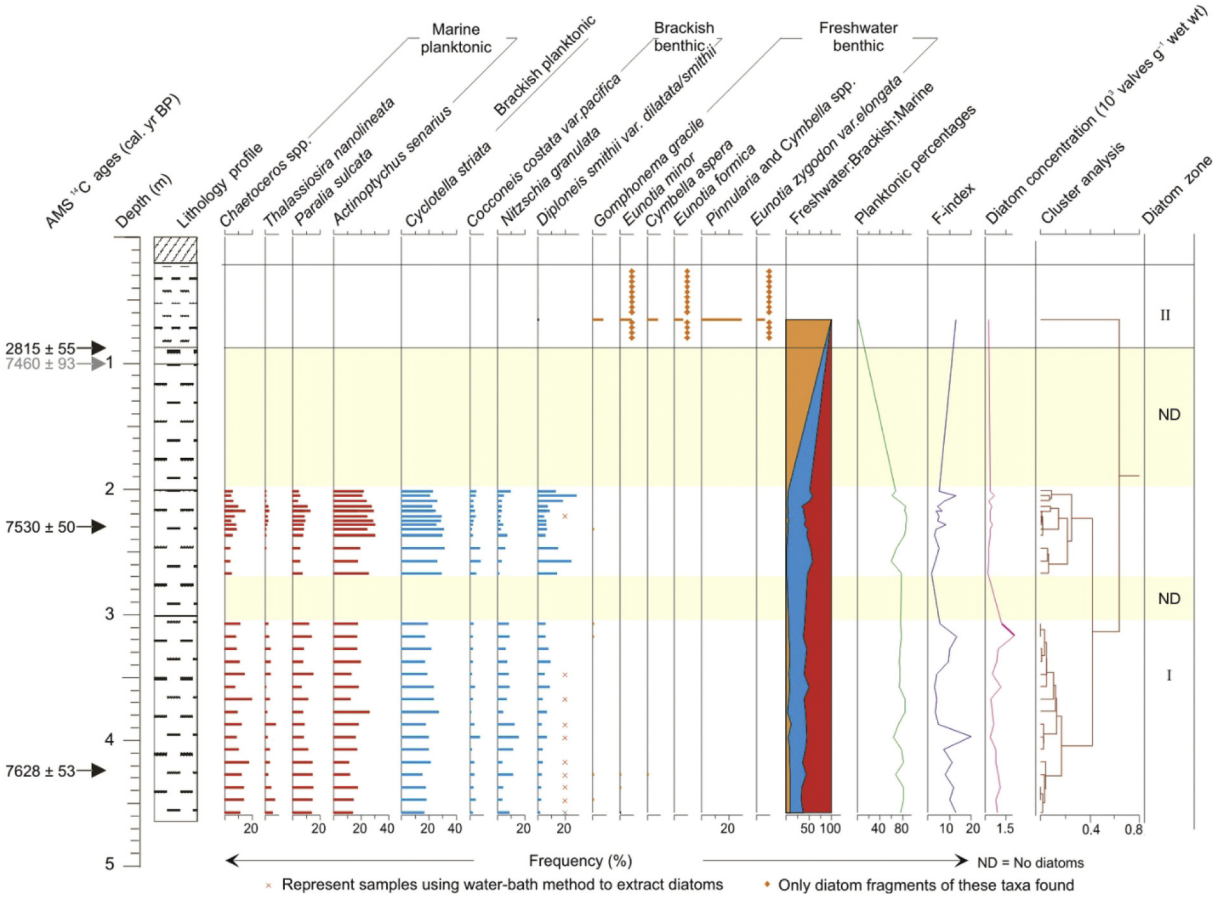

Fig. 4. Diatom taxa in core DTX10 (> 5% relative abundance) with separated into freshwater, brackish and marine species, percentages of planktonic species, F-index and diatom concentration.

bacteria (Müller and Mathesius, 1999; Müller and Voss, 1999; Lamb et al., 2007). The bi-plot of $\delta^{13}C$ to TOC/TN showed that Zone I samples lay in the domain of marine algae or marine particulate organic carbon (POC; Fig. 6B). The bi-plot of $\delta^{15}N$ against TOC/TN reflected a predominant contribution from algae as well (Fig. 6C).

An abrupt increase in TOC (1.07–2.12%, avg. 1.47%), TN (0.10–0.16%, avg. 0.13%) and TOC/TN (9.07–13.50, avg. 11.53) characterised zone II with lower $\delta^{13}C$ (from −25.58‰ to −26.61‰, avg. −26.74‰) and $\delta^{15}N$ (from +1‰ to +4.39‰, avg. +2.25‰), signifying the sudden increase in importance of C_3 terrestrial plants and reflecting the formation of a marsh environment. A shift on the bi-plots of $\delta^{13}C$ and $\delta^{15}N$ vs. TOC/TN implied a mixture of freshwater POC and C_3 plants for samples in Zone II with one exception of marine POC in Zone II_2. The gradual increase in $\delta^{13}C$ and $\delta^{15}N$ from Zone II_1 to II_2, and to II_3, coincided with changes in position in bi-plots of $\delta^{13}C$ and $\delta^{15}N$ against TOC/TN which was interpreted as a slight, but persistent, increase in the importance of marine algae/POC from the bottom to the top of Zone II.

TOC, TN, TOC/TN values increased gradually to maxima of 10.83%, 0.51% and 21.09, respectively, from Zone III to the top of IV where lithology changed to peaty mud, while $\delta^{13}C$ and $\delta^{15}N$ values dropped consistently to minima of −27.76‰ and −0.55‰, respectively. Integrating patterns on the two bi-plots (Fig. 6B and C), Zone III was dominated mostly by terrestrial C_3 plants and secondarily by freshwater algae/POC, while typical terrestrial C_3 plants dominated the organic matter composition of Zone IV. In Zone V, a rapid drop in TOC (avg. 1.34%), TN (avg. 0.14%) and the TOC/TN ratio (avg. 9.13) occurred, with lowest values in subzone V_2 followed by an increase in subzone V_3. The $\delta^{13}C$ values remained depleted except for subzone V_2 (1.25–1.45 m) where they showed peaks, while the $\delta^{15}N$ values increased suddenly and remained high from the bottom to the top. The pattern on the two bi-plots (Fig. 6B and C) suggested an increase in freshwater algae/POC and bacteria in Zone V, especially in Zone V_2 where algae and bacteria dominated.

4.3.2. Core DTX10

In Zone I (from the base to 1.0 m, 7650–7460 cal. yr BP), silt content was 50–74%, the highest values in the profile, with lesser amounts of clay and sand (Fig. 7). Zone II (1.0–0.88 m, 7460–2810 cal. yr BP) was a transitional zone for all proxies. There was a slight and gradual increase in silt content from the bottom to the top, while sand content remained constant. In Zone III (0.88 m to the top, 2810 cal. yr BP to present) both silt and clay content dropped while sand content rose dramatically to 26% on average, with a slight increase in clay and silt content at the top of Zone III_2.

A linear correlation between TOC and TN was found, but two discrete groups were identified (Fig. 6D): the samples in Zone I formed one group and samples in Zone II and III a second. This showed that TN values were mostly controlled by organic matter, but also inorganic nitrogen contributed slightly as shown by the positive TN intercept of 0.035% and 0.09% respectively. Plotting $\delta^{13}C$ against TOC/TN revealed a mixture of two end members of POC/algae/bacteria and C_3 terrestrial plants (Fig. 6E). This explanation was supported by the strongly negative linear correlation between $\delta^{15}N$ and TOC/TN ($r = -0.85$; Fig. 6F). TOC values were 0.42–0.89% (avg. 0.59%) in zone I and TN 0.08–0.14% (avg. 0.10%) (Fig. 7), while TOC/TN ratios were 4.35–7.41 (avg. 5.80). These minimum values were accompanied by the highest $\delta^{13}C$ (from −23.82‰ to −26.32‰, avg. −24.73‰) and $\delta^{15}N$ values (from +3.44‰ to +6.12‰, avg. 4.30‰). Very small increases in TOC, TN and TOC/TN coincided with minor decreases of $\delta^{13}C$ and $\delta^{15}N$ from

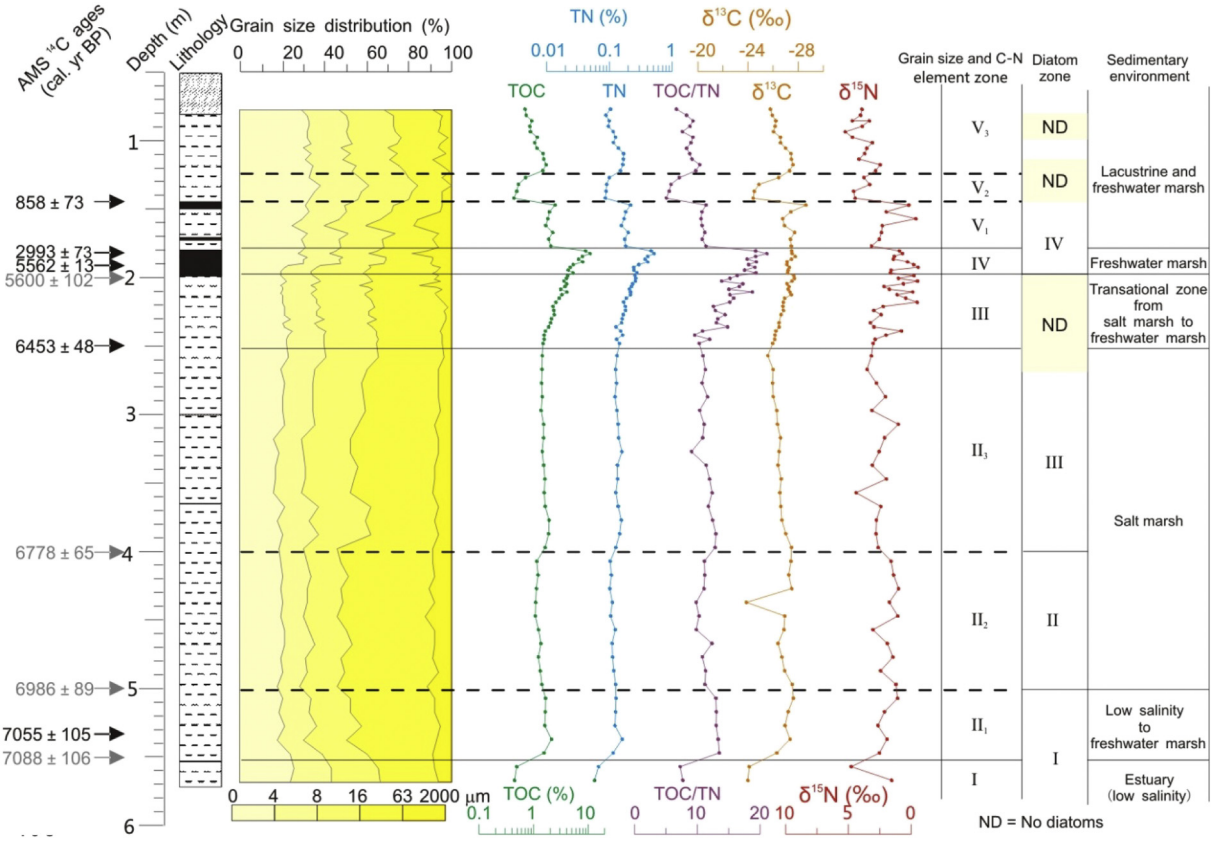

Fig. 5. Lithology and sedimentary parameters of core DTX4, including AMS ^{14}C age, grain size distribution, TOC, TN, TOC/TN, $\delta^{13}C$, $\delta^{15}N$, and interpretation of sedimentary environment.

Zone I_1 to I_3. Integrating patterns on the plots of $\delta^{13}C$ and $\delta^{15}N$ against TOC/TN, a mixture of freshwater and marine algae/POC and bacteria composed the organic matter source for samples in Zone I, with the freshwater algal/POC contribution increasing from Zone I_1 to I_3. In Zone II, TOC and TN values increased rapidly up to 1.79% and 0.14% on average and TOC/TN up to 12.37. On the contrary, $\delta^{13}C$ and $\delta^{15}N$ declined to −27.89‰ and +2.39‰, respectively. Changes in all these proxies reflected an abrupt addition of terrestrial organic matter from C_3 plants, supported by the bi-plots of $\delta^{13}C$ and $\delta^{15}N$ against TOC/TN. In Zone III, this pattern of consistently high TOC, TN and TOC/TN and lower $\delta^{13}C$ and $\delta^{15}N$ continued, with small decreases in these parameters in Zone III_2. On bi-plots of $\delta^{13}C$ and $\delta^{15}N$ vs. TOC/TN, samples of Zone III_1 fell in the region typical of C_3 terrestrial plants and samples of Zone III_2 in the region between C_3 plants and freshwater POC/algae.

5. Discussion

5.1. Sedimentary, morphological and hydrological changes in the East Tiaoxi River Plain

The dominance of marine diatoms and marine algae/POC contribution for the TOC in core DTX10 confirms that there was a high salinity estuary (the Palaeo-Taihu Estuary) in the East Tiaoxi River Plain before ca. 7500 cal. yr BP (Figs. 4, 7; Hong, 1991), in response to rapid early to mid-Holocene sea-level rise (Chappell and Polach, 1991; Bard et al., 1996; Bird et al., 2007; Wang et al., 2012). The high sedimentation accumulation rate up to 2 cm yr^{-1} in core DTX10 during this period signified rapid infilling of this estuary. From ca. 7500 cal. yr BP, freshening occurred at site DTX10 indicated by the increase in organic source from freshwater algae/POC (Zone I_2–I_3 in Fig. 7). At some time after ca. 7500 cal. yr BP, the area around core DTX10 was subaerially exposed until ca. 2800 cal. yr BP, inferred from the sedimentation hiatus and observed pedogenesis (1.0–0.88 m in Figs. 2 and 7). In contrast, the area around core DTX4 changed from estuary to a low-salinity marsh during ca. 7100–7000 cal. yr BP, indicated by dominant organic matter changing from marine algae/POC to freshwater algae/POC and C_3 terrestrial plants (Fig. 5). The estuary at 7100 cal. yr BP was also characterised by low salinity, with the diatom assemblages dominated by salt-tolerant freshwater group of *A. granulata/ambigua*, *P. brevistriata*, *S. construens* and its varieties of *S. construens f. venter* and *S. construens f. construens* (Fig. 3). These diatom taxa are often found in isolation basins (e.g. freshwater lakes formed as sea level falls) (Stabell, 1985), and therefore, their high concentrations indicate that the site DTX4 was in the stage of isolation from seawater during ca. 7100–7000 cal. yr BP. Consequently, we infer that the freshening of the East Tiaoxi River Plain likely started between 7500 and 7100 cal. yr BP, possibly due to coastal development and freshwater discharge from the Yangtze River, benefitting from a warmer and, more importantly, wetter climate during the Holocene Thermal Maximum (Wang et al., 2005). Particularly, *A. granulata* is often found in rivers/lakes in the flood and delta plains in eastern China and has been considered as an indicator of freshwater discharge to estuaries (Chen et al., 2011; Dong et al., 2008; Liu et al., 2012; Wang et al., 2009). We thus suppose high and constant percentages of *A. granulata* during 7100–6500 cal. yr BP in core DTX4 implied the strong freshwater influence of Yangtze River runoff.

At some time after ca. 7000 cal. yr BP, although the marsh was dominated by C_3 plants and strongly influenced by the Yangtze freshwater discharge, penetration of salt water occurred at core DTX4 as percentages of brackish benthic diatom and influence from marine POC/algae increased (Zone II_2 and II_3 in Figs. 5; 6). During this period, the infilling of the Palaeo-Taihu Estuary continued, but at a lower SR of 0.48 cm yr^{-1}. The return of sea water was likely caused by the sudden sea-level rise at ca. 6.8 ± 0.2 ka BP due to the disappearance of the

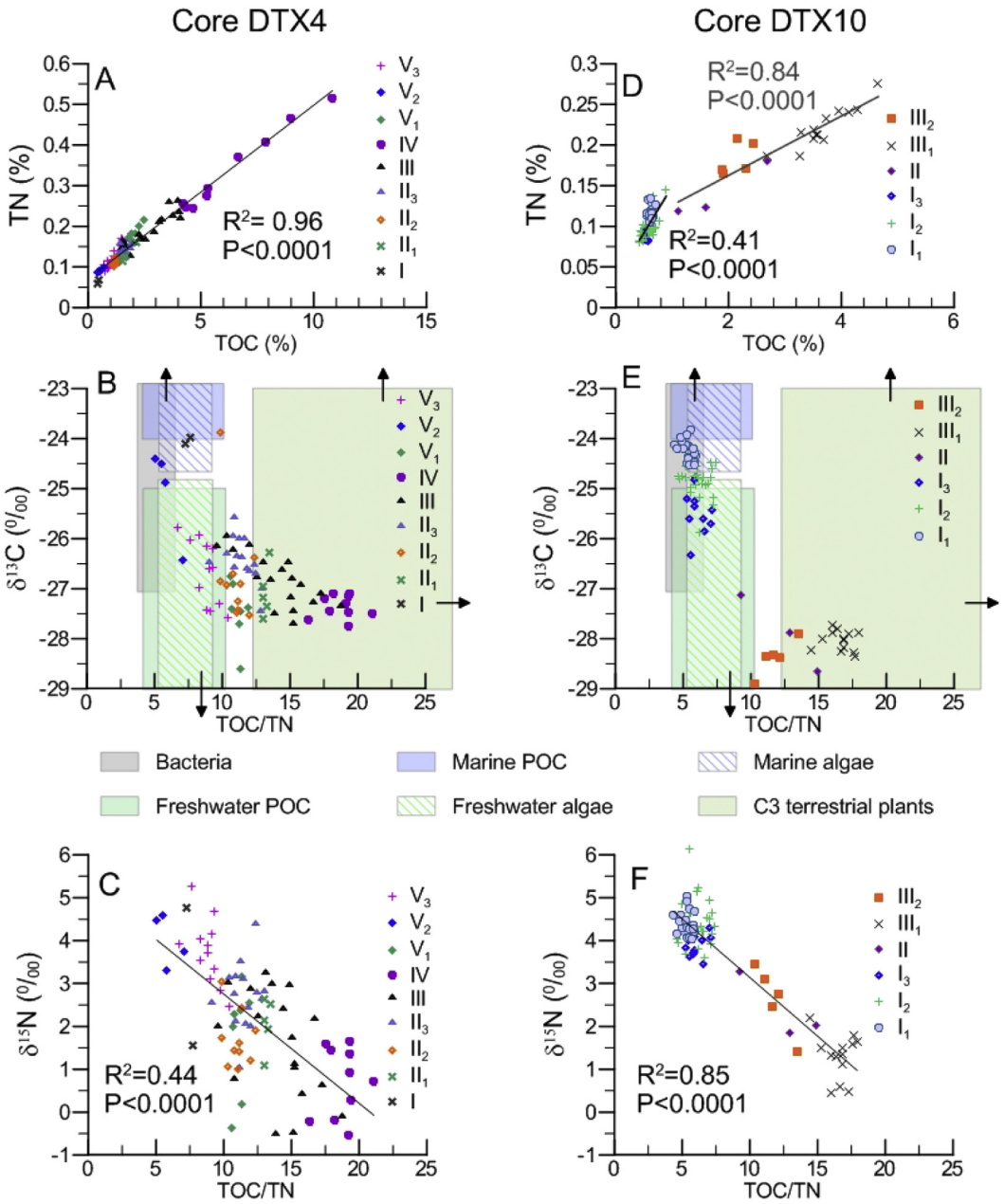

Fig. 6. Correlation between TOC and TN (A and D), biplot of $\delta^{13}C$ values and TOC/TN (B and E), correlation between $\delta^{15}N$ values and TOC/TN (C and F) for core DTX4 (A to C) and DTX10 (D to F), respectively. Regions for different type of organic matter are after Lamb et al. (2007).

west section of the Laurentide ice sheet (Blanchon and Shaw, 1995; Carlson et al., 2007). From ca. 6500 to 5600 cal. yr BP, sea water retreated slowly again and the sedimentary environment transitioned gradually from salt marsh to freshwater marsh in the area near core DTX4, reflected by the composition of organic matter over this period (Fig. 5), while site DTX10 was subaerially exposed (1.0–0.88 m in Fig. 7). Correspondingly, the infilling rate of the Palaeo-Taihu Estuary fell dramatically, likely signifying a process of shrinking due to the stable or slightly declining sea level from ca. 6300 cal. yr BP (Fairbanks, 1989; Bard et al., 1996; Bird et al., 2007; Wang et al., accepted). After ca. 5600 cal. yr BP, the East Tiaoxi River Plain transitioned through a range of environments from stable freshwater marsh (core DTX4) or dry land (core DTX10), characterised by freshwater benthic diatoms and C_3 terrestrial plants respectively (Figs. 3–7). In other words, no sea water penetration occurred and entirely freshwater environments persisted from ca. 5600 cal. yr BP throughout to the present. In terms of the Palaeo-Taihu Estuary, it likely shrank dramatically as it was filled up with sediment.

This study also demonstrates that viable and informative diatom counts can be made using the sodium polytungstate (SPT) density separation technique even on material which has very low diatom concentrations (here, largely as a result of dissolution). There is some indication that there is some preferential recovery of certain taxa (compare adjacent samples using the standard water-bath and SPT method in core DTX10 in Fig. 4, for example for *Diploneis smithii* in Zone I) but there is clearly little systematic difference between the two methods, thus confirming the utility of the approach in such sediments. Results here support the use of SPT as a very useful technique which may have wider application in estuarine and marine sediments, where the option of working on material with well-preserved or abundant diatoms (or other siliceous remains) may simply not be available, and yet may deliver much information of great palaeoecological value, even with poorly preserved assemblages (cf. Ryves et al., 2006, 2009).

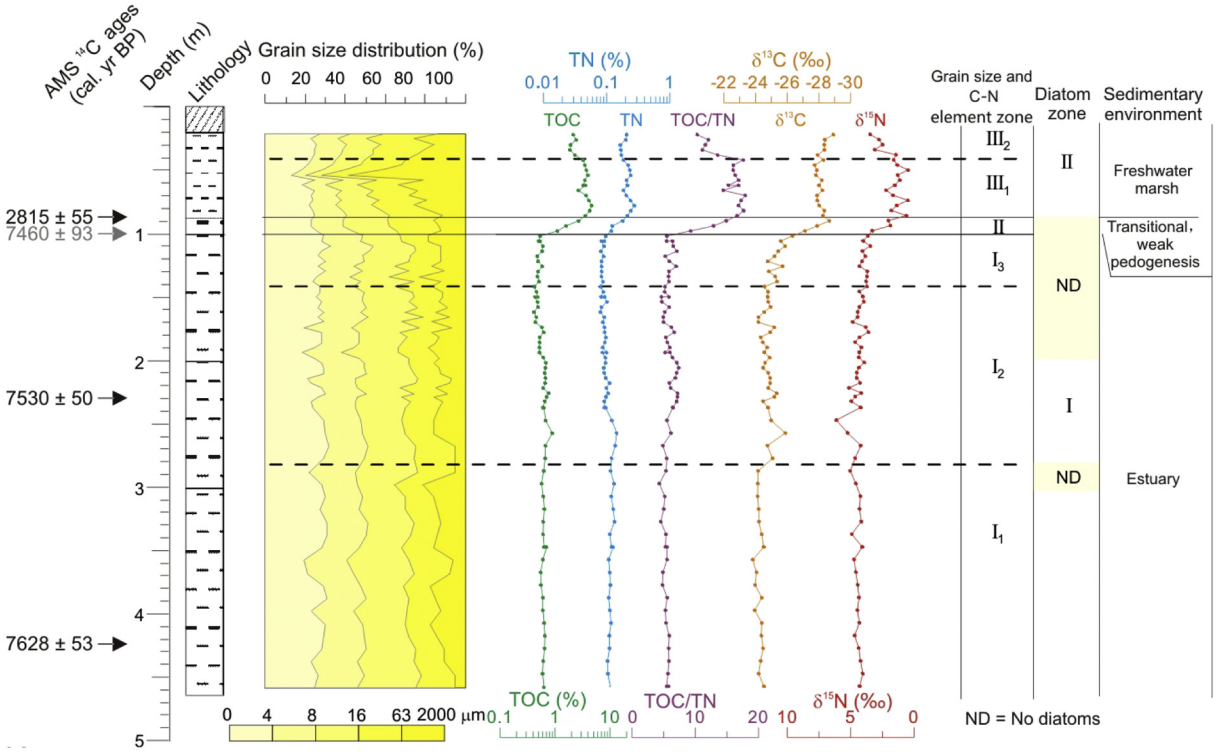

Fig. 7. Lithology and sedimentary parameters of core DTX10, including AMS ^{14}C age, grain size distribution, TOC, TN, TOC/TN, $\delta^{13}C$, $\delta^{15}N$, and sedimentary environments interpretation.

5.2. Environmental changes in the whole Taihu Plain

We recognise six stages for the morphological and hydrologic evolution of the Palaeo-Taihu Estuary according to the multi-proxy analyses in cores DTX4 and DTX10. Before 7500 cal. yr BP, it was a high salinity estuary; 7500–7100 cal. yr BP, a low salinity estuary influenced strongly by the Yangtze freshwater discharge; 7100–7000 cal. yr BP, it developed into a low salinity to freshwater marsh; 7000–6500 cal. yr BP, salt water penetrated into the marsh; 6500–5600 cal. yr BP, gradual retreat of marine influence; and from 5600 cal. yr BP, stable freshwater conditions. A similar history of hydrologic change can be inferred from the stratigraphic transections across the Taihu Plain (Fig. 8).

Estuarine facies dominated before 7500 cal. yr BP in multiple cores including 97C, 97A, DS, JLQ, GT and XL in the palaeo-Taihu Estuary (Fig. 8A; references for these cores are in Supplementary Table 1), due to rapid sea-level rise in the early Holocene (Wang et al., 2012). The sedimentary facies then turned into tidal flat in these cores around 7500 cal. yr BP owing to the infilling of the estuary (Fig. 8A). Brackish tidal flat conditions also occurred in other cores like ZX-1, GFL and TL in the east Taihu Plain (Fig. 8C). As the relative sea level reached approximately −6 m at 7500 cal. yr BP (Wang et al., 2012), the late Pleistocene interfluve terrace T1 region (including around Shanghai City) was a shallow sea environment due to this transgressive phase (Li et al., 2002; Zong, 2004; Wang et al., 2012, 2013). No sea water penetration occurred throughout the Holocene in the region of the late Pleistocene interfluve terrace T3 (Fig. 1C) where palaeo-altitude was the highest during the LGM (as recorded in core E2, YJD, CD, CXS and SQ; Fig. 8B and C). The central Taihu Plain was isolated from western uplands due to sea water inundation through the Palaeo-Taihu Estuary at ca. 7500 cal. yr BP (Fig. 9A).

The marine regression at ca. 7500–7000 cal. yr BP recorded in core DTX4 and DTX10 was also seen in cores in the Palaeo-Taihu Estuary (e.g. cores JLQ, GT and WJB; Fig. 8A). In the central Taihu Plain, low salinity to freshwater marshes developed at ca. 7600–7120 cal. yr BP in core WJB (Fig. 8B), indicated by reduced concentration of marine dinoflagellate cysts and *Chenopodiaceae* pollen (Qin et al., 2011). Consequently, this sea water regression event promoted the rapid expansion of low salinity to freshwater marshes, especially in the area of the Palaeo-Taihu valley (Fig. 9B).

Evidence for sea water penetration after 7000 cal. yr BP was found in several sediment cores (e.g. PW, WJB, MJB) in the central Taihu Plain (Fig. 8B) in addition to those in the Palaeo-Taihu Estuary (Fig. 8A). Moreover, this marine transgression reached areas where no sea water influence was observed in the records before. For example, the foraminifera *Ammonia compressiuscula* and *Ammonia cff. sobrina*, which prefer brackish tidal flat environments, occurred for the first time in the peat layer dated at ca. 7000 cal. yr BP at site LTD, located at the head of the Palaeo-Taihu valley, northwest of the Taihu Plain (Li et al., 2008; Fig. 8B). Marine and brackish diatom species, marine species of dinoflagellate cysts and foraminifera were only found at 50–90 cm (dated at ca. 7000 cal. yr BP) in core W1 in the north part of Taihu Lake (Figs. 8B and 9C; Chang et al., 1994, Wang et al., 2001). Sea water also inundated the low salinity marsh around core PW in the south east Taihu Plain at some time after 7200 cal. yr BP (Fig. 8B; Zong et al., 2011; Innes et al., 2014). Therefore, the transgression during ca. 7000–6500 cal. yr BP influenced a large area, including the innermost Taihu Plain, through low-lying area such as the Palaeo-Taihu valley (Fig. 9C). Low salinity marsh then returned from ca. 6200 to 5600 cal. yr BP at sites LTD, W1, PW and DTX4 (Fig. 8), and thereafter stable freshwater conditions in the central Taihu Plain developed completely after ca. 5600 cal. yr BP, likely indicating the closure of the Palaeo-Taihu Estuary (Fig. 9D).

5.3. Role of hydrological environments on the development of rice farming

Rice growth is susceptible to salinity conditions and demands suitable water depth, in addition to warm and humid climate (Zeng et al., 2003; Yu et al., 2000; Chen et al., 2005; Innes et al., 2009, 2014; Patalano et al., 2015). The Taihu Plain was semi-encircled by sea water before ca. 7500 cal. yr BP (Fig. 9A), corresponding with no sedentary

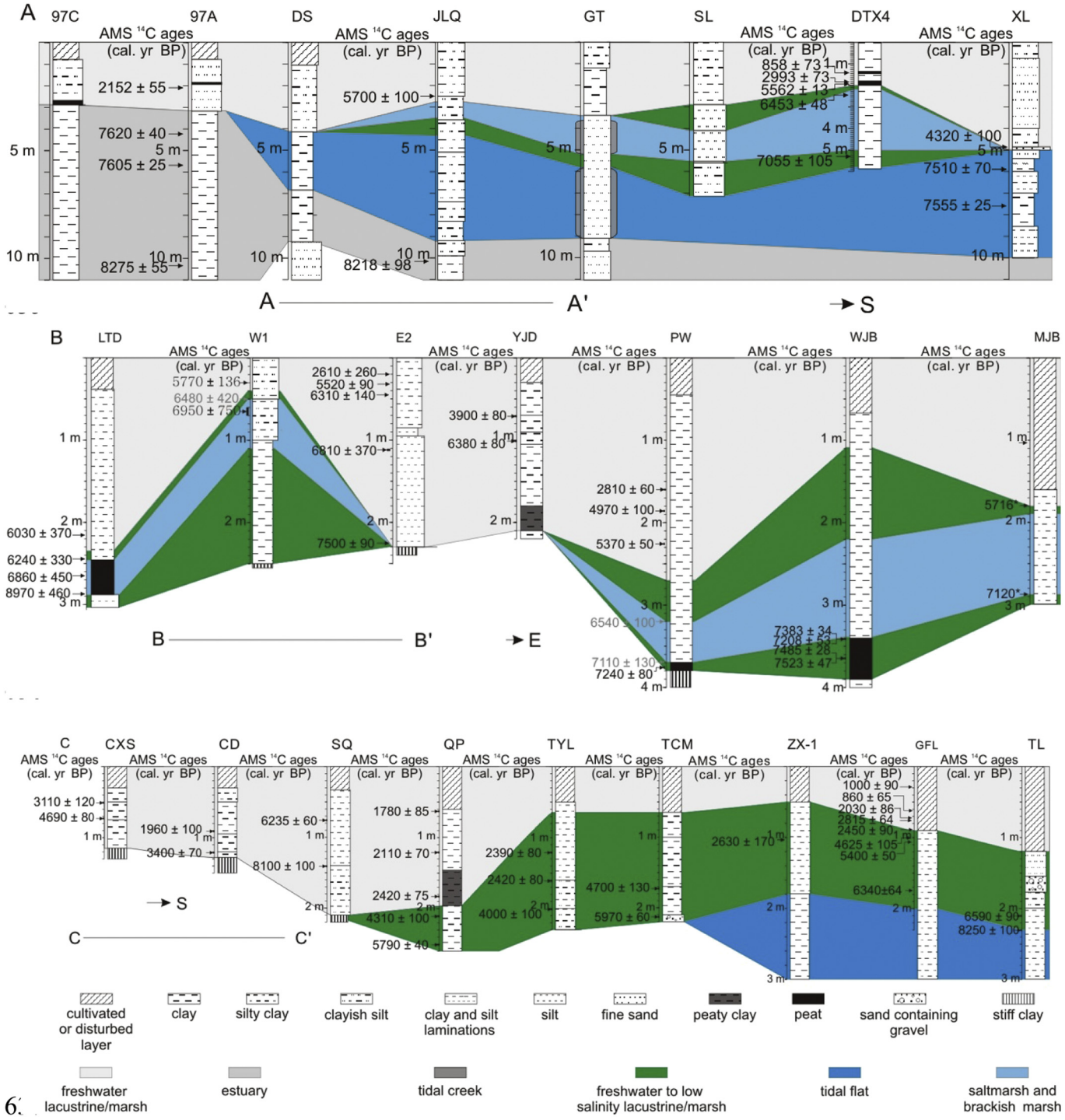

Fig. 8. Stratigraphic transections of collected cores, including sections A-A′ (A) and B-B′ (B) and C-C′ (C). In section A-A′, core 97C is after Ding (2004), core 97A after Zhou and Zheng (2000), and core DS, JLQ, GT and SL are after Yan and Huang (1987) and Hong (1991), and core XL is after Liu et al. (2015). In section B-B′, site LTD is after Li et al. (2008), core W1 after Chang et al. (1994) and Wang et al. (2001), core E2 after Wang et al. (2001), core YJD and PW after Zong et al. (2011, 2012b) and Innes et al. (2014), core WJB after Qin et al. (2011) and MJB after Long et al. (2014). In section C-C′, core CXS, CD and TYL are after Zong et al. (2012b), core SQ, TCM and TL after Zong et al. (2011), core QP after Atahan et al. (2008) and Itzstein-Davey et al. (2007), ZX-1 after Chen et al. (2005) and Tao et al. (2006) and core GEL after Wang et al. (2012). 0 m is the start depth for each core. Ages in black are from references for each core and ages in grey black are linearly interpolated based on "Clam" (Blaauw, 2010).

Neolithic settlements and no remains of rice cultivation (Mo et al., 2011). Concurrent with withdrawal of sea water and expansion of low salinity and freshwater marshes between ca. 7500 cal. yr BP and ca. 7000 cal. yr BP, rice cultivation began (Cao et al., 2006; Fuller et al., 2007; Mo et al., 2011; Zong et al., 2011) and the Majiabang culture developed in the Taihu Plain, in addition to benefits of heat and precipitation provided by the optimum climate (Chen et al., 2005; Wang et al., 2005). However, no rapid advance in rice cultivation or productivity, or in the number of Neolithic sites, occurred during the late Majiabang and early Songze period. This is likely due to the lack of adequate freshwater supply, because the central Taihu plain was isolated from the western uplands by the Taihu-Palaeo Estuary until at

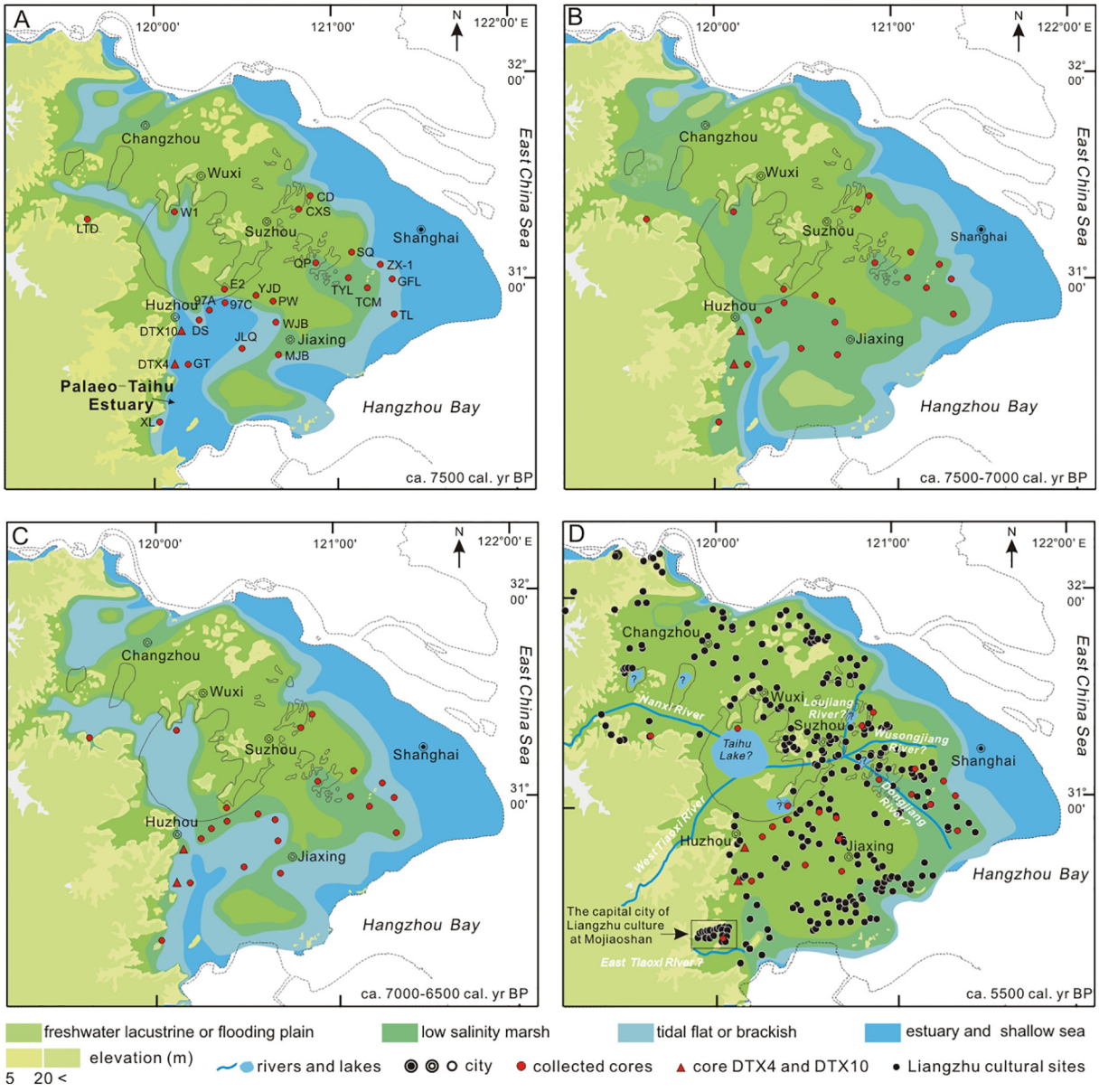

Fig. 9. Palaeogeographic map for the Taihu Plain before ca. 7500 cal. yr BP (A), during ca. 7500–7000 cal. yr BP (B), during ca. 7000–6500 cal. yr BP (C), and at ca. 5500 cal. yr BP (D). Rivers in (D) are based on Hong (1991), and the possible formation of Taihu Lake is based on Wang et al. (2001). The number of Liangzhu (5500–4500 cal. yr BP) cultural sites grew rapidly to 461, while it is only 78 and 93 during the Majiabang (7000–5800 cal. yr BP) and Songze (5800–5500 cal. yr BP) period, respectively (from Zheng, 2002; Chen, 2002; Xu, 2015).

around 5600 cal. yr BP (Fig. 9), and hence no river discharge from the western uplands entered the central Taihu plain.

We further suggest that the freshening of the East Tiaoxi River Plain or the shrinkage/closure of the Palaeo-Taihu Estuary at ca. 5600 cal. yr BP, was critical for the rapid expansion of rice agriculture across the whole Taihu Plain during the Liangzhu period (Fig. 9D), in the context of deteriorating climate conditions compared with the Majiabang and Songze period (Wang et al., 2005; Innes et al., 2014). Firstly, the shrinkage/closure of the Palaeo-Taihu Estuary, which is supported by extensive distribution of Liangzhu cultural sites in the Tiaoxi River Plain (Zheng, 2002), prevented the intrusion of sea water from Hangzhou Bay into the Taihu Plain, allowing freshwater conditions, particularly in the southern and western parts. Secondly, it restricted the discharge of freshwater from the western uplands (e.g. the west Tiaoxi river) into the Hangzhou Bay, and instead, forced this freshwater to flow eastwards, likely forming three previously existing rivers: the Loujiang River, the Wusongjiang River and the Dongjiang River (Fig. 9D; Hong, 1991). This increasing density of the river network would provide an increasing area of freshwater wetlands available to be transformed into rice paddies and greater quantity of fresh water for the east Taihu Plain. This conjecture is supported by the fact that the area of rice paddy fields excavated in several archeological sites recently was several times larger during the Liangzhu period than during the Majiabang and Songze period, and were connected to natural and artificial creeks, instead of wells and ponds, which had stronger capability of water storage (Cao et al., 2007; Hu et al., 2013; Zheng et al., 2014; Zhuang et al., 2014). Thirdly, new or enlarged freshwater marsh environments of the East Tiaoxi River Plain would have supplied additional freshwater wetland resources. Lastly, water level rise, in response to sea-level rise after the Taihu Plain was separated from the Hangzhou Bay and the East China Sea, would also encourage formation of freshwater wetlands (Hong, 1991; Chen et al., 1997). All these advantages together would have increased opportunity for domesticated rice cultivation in the whole Taihu Plain and rice productivity, supporting the

continuous and dramatic advancement of the Liangzhu culture.

We also speculate that the terrestrialisation and freshening of the East Tiaoxi River Plain may have facilitated communication between the north and east Taihu Plain, with the capital city of Liangzhu at Mojiaoshan, southwest of Taihu Plain (Fig. 9D) and even with areas south of Hangzhou Bay (Chen, 2015; Xu, 2015), given the barrier that the Palaeo-Taihu Estuary would have represented. Such easier communication would support the development and flourishing of the Liangzhu capital city. In return, the capital city would be act as a hub for advanced technology and cultural innovation, promoting the further expansion of rice farming and cultural development in the region over the Liangzhu period.

6. Conclusions

A multiproxy sedimentological analysis combining chronological, lithological, geochemical and biological analyses of two sediment cores (DTX4 and DTX10) collected from the East Tiaoxi River Plain, southern Yangtze delta Plain, have shed light on changes in landscape and hydrology in this region over the last 7500 years. Before ca. 7500 cal. yr BP, the Palaeo-Taihu Estuary existed along the present day East Tiaoxi River Plain. It infilled rapidly by ca. 7500 cal. yr BP and was characterised by low salinity conditions, because of the large supply of freshwater from the Yangtze River. Sea water, however, again penetrated the East Tiaoxi River Plain after ca. 7000 cal. yr BP due to an abrupt sea-level rise, and a salt marsh environment developed. This transgression was also recorded in other parts of the Taihu Plain where no sea water influence occurred before, hence, it was possibly the largest sea-level transgression during the Holocene, based on the synthesis of a large number of hydrological and environmental records from the region. After ca. 6500 cal. yr BP, sea-water penetration gradually declined and infilling rate of the Palaeo-Taihu Estuary fell owing to slowing sea-level rise. The dramatic shrinkage/closure of the Palaeo-Taihu Estuary occurred after ca. 5600 cal. yr BP, corresponding to the formation of stable freshwater marsh (or subaerial land) conditions in the East Tiaoxi River Plain.

Geomorphological and hydrological changes in the East Tiaoxi River Plain played an important role in the rise of rice cultivation and development of Neolithic cultures across the Taihu Plain. Especially, the freshening of the East Tiaoxi River Plain or its terrestrialisation after ca. 5600 cal. yr BP, was likely one critical precondition encouraging rapid increase of rice productivity (and so cultural development) during the Liangzhu period.

Supplementary data to this article can be found online at https://doi.org/10.1016/j.palaeo.2018.03.012.

Acknowledgments

This study was supported by the National Natural Science Foundation of China (Grant No. 41576042) and the China Scholarship Council Postgraduate Scholarship Program, which allowed TC spending a year at Loughborough University. We are grateful to two anonymous reviewers for their helpful comments.

References

Atahan, P., Itzstein-Davey, F., Taylor, D., Dodson, J., Qin, J., Zheng, H., Brooks, A., 2008. Holocene-aged sedimentary records of environmental changes and early agriculture in the lower Yangtze, China. Quat. Sci. Rev. 27, 556–570.

Bard, E., Hamelin, B., Arnold, M., Montaggioni, L., Cabioch, G., Faure, G., Rougerie, F., 1996. Deglacial sea-level record from Tahiti corals and the timing of global meltwater discharge. Nature 382, 241–244.

Battarbee, R.W., Kneen, M.J., 1982. The use of electronically counted microsphere sin absolute diatom analysis. Limnol. Oceanogr. 27, 184–188.

Battarbee, R.W., Jones, V.J., Flower, R.J., Cameron, N.G., Bennion, H., Carvalho, L., Juggins, S., 2001. Diatoms. In: Smol, J.P., Birks, H.J.B., Last, W.M., Bradley, R.S., Alverson, K. (Eds.), Tracking Environmental Change Using Lake Sediments: Terrestrial, Algal, and Siliceous Indicators. Springer Netherlands, Dordrecht, pp. 155–202.

Beuselinck, L., Govers, G., Poesen, J., Degraer, G., Froyen, L., 1998. Grain-size analysis by laser diffractometry: comparison with the sieve-pipette method. Catena 32, 193–208.

Bird, M., Fifield, L., Teh, T., Chang, C., Shirlaw, N., Lambeck, K., 2007. An inflection in the rate of early mid-Holocene eustatic sea-level rise: a new sea-level curve from Singapore. Estuar. Coast. Shelf Sci. 71, 523–536.

Blaauw, M., 2010. Methods and code for 'classical' age-modelling of radiocarbon sequences. Quat. Geochronol. 5, 512–518.

Blanchon, P., Shaw, J., 1995. Reef drowning during the last deglaciation: evidence for catastrophic sea-level rise and ice-sheet collapse. Geology 23, 4–8.

Cao, Z.H., Ding, J.L., Hu, Z.Y., Knicker, H., Kögel-Knabner, I., Yang, L.Z., Yin, R., Lin, X.G., Dong, Y.H., 2006. Ancient paddy soils from the Neolithic age in China's Yangtze River Delta. Naturwissenschaften 93, 232–236.

Cao, Z.H., Yang, L.Z., Lin, X.G., Hu, Z.Y., Dong, Y.H., Zhang, G.Y., Lu, Y.C., Yin, R., Wu, Y.L., Ding, J.L., Zheng, Y.F., 2007. Morphological characteristics of paddy fields, paddy soil profile, phytolith and fossil rice grain of the Neolithic age in Yangtze river delta. Acta Pedol. Sin. 44, 838–847 (in Chinese, with English abstract).

Carlson, A.E., Clark, P.U., Raisbeck, G.M., Brook, E.J., 2007. Rapid Holocene deglaciation of the Labrador sector of the Laurentide ice sheet. J. Clim. 20, 5126–5133.

Chang, W.Y.B., Xu, X.M., Yang, J.R., Liu, J.L., 1994. Evolution in Taihu Lake ecosystem as evidence of changes in sediment profiles. J. Lake Sci. 6, 217–226.

Chappell, J., Polach, H., 1991. Post-glacial sea-level rise from a coral record at Huon Peninsula, Papua New Guinea. Nature 349, 147–149.

Chen, J., 2002. Neolithic Cultures in the Yangtze Delta, China and Their Environments. East China Normal University, China (PhD Thesis, in Chinese, with English abstract).

Chen, J., 2015. The Formation of the Songze Culture. Relics from South. 1. pp. 57–65 (in Chinese, with English abstract).

Chen, Z., Hong, X., Li, S., Wang, L., Shi, X., 1997. Study of archaeology-related environment evolution of Taihu Lake in southern Chang Jiang Delta Plain. Acta Geograph. Sin. 52, 131–137 (in Chinese, with English abstract).

Chen, Z., Wang, Z., Schneiderman, J., Taol, J., Cail, Y., 2005. Holocene climate fluctuations in the Yangtze delta of eastern China and the Neolithic response. The Holocene 15, 915–924.

Chen, Z.Y., Zong, Y.Q., Wang, Z.H., Wang, H., Chen, J., 2008. Migration patterns of Neolithic settlements on the abandoned Yellow and Yangtze River deltas of China. Quat. Res. 70, 301–314.

Chen, X., Yang, X., Dong, X., Liu, Q., 2011. Nutrient dynamics linked to hydrological condition and anthropogenic nutrient loading in Chaohu Lake (southeast China). Hydrobiologia 661, 223–234.

Ding, Y.F., 2004. Deposit Record of Climate and Environmental Changes of Taihu Lake Since 10,000 a. East China Normal University, China (Master Thesis, in Chinese, with English abstract).

Dong, X., Bennion, H., Battarbee, R., Yang, X., Yang, H., Liu, E., 2008. Tracking eutrophication in Taihu Lake using the diatom record: potential and problems. J. Paleolimnol. 40, 413–429.

Fairbanks, R.G., 1989. A 17,000-year glacio-eustatic sea level record: influence of glacial melting rates on the Younger Dryas event and deep-ocean circulation. Nature 342, 637–642.

Fan, Y.P., 2011. On the Development of Rice Farming in Tailake Area During the Neolithic Age of China. Nanjing Agriculture University, China (Master Thesis, in Chinese, with English abstract).

Fuller, D.Q., Harvey, E., LING, Q., 2007. Presumed domestication? Evidence for wild rice cultivation and domestication in the fifth millennium BC of the Lower Yangtze region. Antiquity 81, 316–331.

Gell, P., Tibby, J., Little, F., Baldwin, D., Hancock, G., 2007. The impact of regulation and salinisation on floodplain lakes: the lower River Murray, Australia. Hydrobiologia 591, 135–146.

Grönlund, T., 1993. Diatoms in surface sediments of the Gotland Basin in the Baltic Sea. Hydrobiologia 269-270, 235–242.

Hasle, G.R., Syvertsen, E.E., 1996. Chapter 2-marine diatoms. In: Identifying Marine Diatoms & Dinoflagellates, pp. 5–385.

Hong, X., 1991. Origin and evolution of the Taihu Lake. Mar. Geol. Quat. Geol. 11, 87–99 (in Chinese, with English abstract).

Hu, L., Chao, Z., Gu, M., Li, F., Chen, L., Liu, B., Li, X., Huang, Z., Li, Y., Xing, B., 2013. Evidence for a Neolithic Age fire-irrigation paddy cultivation system in the lower Yangtze River Delta, China. J. Archaeol. Sci. 40, 72–78.

Innes, J.B., Zong, Y., Chen, Z., Chen, C., Wang, Z., Wang, H., 2009. Environmental history, palaeoecology and human activity at the early Neolithic forager/cultivator site at Kuahuqiao, Hangzhou, eastern China. Quat. Sci. Rev. 28, 2277–2294.

Innes, J.B., Zong, Y., Wang, Z., Chen, Z., 2014. Climatic and palaeoecological changes during the mid-to Late Holocene transition in eastern China: high-resolution pollen and non-pollen palynomorph analysis at Pingwang, Yangtze coastal lowlands. Quat. Sci. Rev. 99, 164–175.

Itzstein-Davey, F., Atahan, P., Dodson, J., Taylor, D., Zheng, H., 2007. Environmental and cultural changes during the terminal Neolithic: Qingpu, Yangtze delta, eastern China. The Holocene 17, 875–887.

Jiang, L., Liu, L., 2006. New evidence for the origins of sedentism and rice domestication in the Lower Yangzi River, China. Antiquity 80, 355–361.

Juggins, S., 1991–2009. C2 Data Analysis. Newcastle University, Newcastle Available at: http://www.staff.ncl.ac.uk/staff/stephen.juggins/software/C2Home.htm.

Juggins, S., 2013. Quantitative reconstructions in palaeolimnology: new paradigm or sick science? Quat. Sci. Rev. 64, 20–32.

Kilham, P., 1990. Ecology of *Melosira* species in the Great Lakes of Africa. In: Tilzer, M.M., Serruya, C. (Eds.), Large Lakes: Ecological Structure and Function. Springer Berlin Heidelberg, Berlin, Heidelberg, pp. 414–427.

Krammer, K., Lange-Bertalot, H., 1986. Bacillariophyceae. 1: Teil: Naviculaceae. In: Ettl,

H., Gärtner, G., Gerloff, J., Heynig, H., Mollenhauer, D. (Eds.), Süsswasserflora von Mitteleuropa, Band 2/1. Gustav Fischer Verlag, Stuttgart, New York.
Krammer, K., Lange-Bertalot, H., 1988. Bacillariophyceae. 2: Teil: Bacillariaceae, Epithemiaceae, Surirellaceae. In: Ettl, H., Gärtner, G., Gerloff, J., Heynig, H., Mollenhauer, D. (Eds.), Süsswasserflora von Mitteleuropa, Band 2/2. Gustav Fischer Verlag, Stuttgart, New York.
Krammer, K., Lange-Bertalot, H., 1991a. Bacillariophyceae. 3: Teil: Centrales, Fragilariaceae, Eunotiaceae. In: Ettl, H., Gärtner, G., Gerloff, J., Heynig, H., Mollenhauer, D. (Eds.), Süsswasserflora von Mitteleuropa, Band 2/3. Gustav Fischer Verlag, Stuttgart, Jena.
Krammer, K., Lange-Bertalot, H., 1991b. Bacillariophyceae. 4: Teil: Achnanthaceae. In: Ettl, H., Gärtner, G., Gerloff, J., Heynig, H., Mollenhauer, D. (Eds.), Süsswasserflora von Mitteleuropa, Band 2/4. Gustav Fischer Verlag, Stuttgart, Jena.
Lamb, A.L., Vane, C.H., Wilson, G.P., Rees, J.G., Moss-Hayes, V.L., 2007. Assessing $\delta^{13}C$ and C/N ratios from organic material in archived cores as Holocene sea level and palaeoenvironmental indicators in the Humber Estuary, UK. Mar. Geol. 244, 109–128.
Lawler, A., 2009. Beyond the Yellow River: how China became China. Science 325, 930–935.
Leng, M.J., Lewis, J.P., 2017. C/N ratios and carbon isotope composition of organic matter in estuarine environments. In: Weckström, K., Saunders, K.M., Gell, P.A., Skilbeck, C.G. (Eds.), Applications of Paleoenvironmental Techniques in Estuarine Studies. Springer Netherlands, Dordrecht, pp. 213–237.
Li, C.X., Chen, Q.Q., Zhang, J.Q., Yang, S., Fan, D., 2000. Stratigraphy and paleoenvironmental changes in the Yangtze delta during the Late Quaternary. J. Asian Earth Sci. 18, 453–469.
Li, C.X., Wang, P.X., Sun, H.P., Zhang, J.Q., Fan, D., Deng, B., 2002. Late Quaternary incised-valley fill of the Yangtze delta (China): its stratigraphic framework and evolution. Sediment. Geol. 152, 133–158.
Li, L., Zhu, C., Lin, L., Zhao, Q., Shi, G., Zhu, H., 2008. Transgression records between 7500–5400 BC on the stratum of the Luotuodun site in Yixing, Jiangsu province. Acta Geograph. Sin. 63, 1189–1197.
Liu, L., Chen, X., 2012. The Archaeology of China: From the Late Paleolithic to the Early Bronze Age. Cambridge World Archaeology, Cambridge.
Liu, Q., Yang, X., Anderson, N.J., Liu, E., Dong, X., 2012. Diatom ecological response to altered hydrological forcing of a shallow lake on the Yangtze floodplain, SE China. Ecohydrology 5, 316–325.
Liu, Y., Sun, Q., Thomas, I., Zhang, L., Finlayson, B., Zhang, W., Chen, J., Chen, Z., 2015. Middle Holocene coastal environment and the rise of the Liangzhu City complex on the Yangtze delta, China. Quat. Res. 84, 326–334.
Long, T., Qin, J., Atahan, P., Mooney, S., Taylor, D., 2014. Rising waters: new geoarchaeological evidence of inundation and early agriculture from former settlement sites on the southern Yangtze delta, China. The Holocene 24, 546–558.
Meyers, P.A., 2003. Applications of organic geochemistry to paleolimnological reconstructions: a summary of examples from the Laurentian Great Lakes. Org. Geochem. 34, 261–289.
Middelburg, J.J., Nieuwenhuize, J., 1998. Carbon and nitrogen stable isotopes in suspended matter and sediments from the Schelde Estuary. Mar. Chem. 60, 217–225.
Mo, D., Zhao, Z., Xu, J., Li, M., 2011. Holocene environmental changes and the evolution of the neolithic cultures in China. In: Martini, P.I., Chesworth, W. (Eds.), Landscapes and Societies: Selected Cases. Springer Netherlands, Dordrecht, pp. 299–319.
Müller, A., Mathesius, U., 1999. The palaeoenvironments of coastal lagoons in the southern Baltic Sea, I. The application of sedimentary C_{org}/N ratios as source indicators of organic matter. Palaeogeogr. Palaeoclimatol. Palaeoecol. 145, 1–16.
Müller, A., Voss, M., 1999. The palaeoenvironments of coastal lagoons in the southern Baltic Sea, II. $\delta^{13}C$ and $\delta^{15}N$ ratios of organic matter—sources and sediments. Palaeogeogr. Palaeoclimatol. Palaeoecol. 145, 17–32.
Owen, R.B., Crossley, R., 1992. Spatial and temporal distribution of diatoms in sediments of Lake Malawi, Central Africa, and ecological implications. J. Paleolimnol. 7, 55–71.
Patalano, R., Wang, Z., Leng, Q., Liu, W., Zheng, Y., Sun, G., Yang, H., 2015. Hydrological changes facilitated early rice farming in the lower Yangtze River Valley in China: a molecular isotope analysis. Geology 43.
Qin, J., Taylor, D., Atahan, P., Zhang, X., Wu, G., Dodson, J., Zheng, H., Itzstein-Davey, F., 2011. Neolithic agriculture, freshwater resources and rapid environmental changes on the lower Yangtze, China. Quat. Res. 75, 55–65.
Reimer, P.J., Baillie, M.G.L., Bard, E., Bayliss, A., Beck, J.W., Blackwell, P.G., Ramsey, C.B., Buck, C.E., Burr, G.S., Edwards, R.L., 2009. IntCal09 and Marine09 radiocarbon age calibration curves, 0–50,000 years cal. BP. Radiocarbon 51, 1111–1150.
Renberg, I., 1990. A procedure for preparing large sets of diatom slides from sediment cores. J. Paleolimnol. 4, 87–90.
Ryu, E., Yi, S., Lee, S.-J., 2005. Late Pleistocene-Holocene paleoenvironmental changes inferred from the diatom record of the Ulleung Basin, East Sea (sea of Japan). Mar. Micropaleontol. 55, 157–182.
Ryves, D.B., Juggins, S., Fritz, S.C., Battarbee, R.W., 2001. Experimental diatom dissolution and the quantification of microfossil preservation in sediments. Palaeogeogr. Palaeoclimatol. Palaeoecol. 172, 99–113.
Ryves, D.B., Clarke, A.L., Appleby, P.G., Amsinck, S.L., Jeppesen, E., Landkildehus, F., Anderson, N.J., 2004. Reconstructing the salinity and environment of the Limfjord and Vejler. Can. J. Fish. Aquat. Sci. 61, 1988–2006 (1919).
Ryves, D.B., Battarbee, R.W., Juggins, S., Fritz, S.C., Anderson, N.J., 2006. Physical and chemical predictors of diatom dissolution in freshwater and saline lake sediments in North America and West Greenland. Limnol. Oceanogr. 51, 1355–1368.
Ryves, D.B., Battarbee, R.W., Fritz, S.C., 2009. The dilemma of disappearing diatoms: incorporating diatom dissolution data into palaeoenvironmental modelling and reconstruction. Quat. Sci. Rev. 28, 120–136.
Song, B., Li, Z., Saito, Y., Okuno, J.I., Li, Z., Lu, A., Hua, D., Li, J., Li, Y., Nakashima, R., 2013. Initiation of the Changjiang (Yangtze) delta and its response to the mid-Holocene sea level change. Palaeogeogr. Palaeoclimatol. Palaeoecol. 388, 81–97.
Stabell, B., 1985. The development and succession of taxa within the diatom genus Fragilaria Lyngbye as a response to basin isolation from the sea. Boreas 14, 273–286.
Stanley, D.J., 2000. Radiocarbon dates in China's Holocene Yangtze delta: record of sediment storage and reworking, not timing of deposition. J. Coast. Res. 16, 1126–1132.
Stuiver, M., Reimer, P.J., Reimer, R., 2015. CALIB: Radiocarbon Calibration. http://calib.qub.ac.uk/calib/ (September 2015).
Tada, R., Irino, T., Koizumi, I., 1999. Land-ocean linkages over orbital and millennial timescales recorded in Late Quaternary sediments of the Japan Sea. Paleoceanography 14, 236–247.
Tao, J., Chen, M.T., Xu, S., 2006. A Holocene environmental record from the southern Yangtze River delta, eastern China. Palaeogeogr. Palaeoclimatol. Palaeoecol. 230, 204–229.
Thornton, S.F., McManus, J., 1994. Application of organic carbon and nitrogen stable isotope and C/N ratios as source indicators of organic matter provenance in estuarine systems: evidence from the Tay Estuary, Scotland. Estuar. Coast. Shelf Sci. 38, 219–233.
Vos, P.C., de Wolf, H., 1993. Diatoms as a tool for reconstructing sedimentary environments in coastal wetlands; methodological aspects. Hydrobiologia 269, 285–296.
Wang, J., Chen, X., Zhu, X.H., Liu, J.L., Chang, W.Y.B., 2001. Taihu Lake, lower Yangtze drainage basin: evolution, sedimentation rate and the sea level. Geomorphology 41, 183–193.
Wang, Y., Cheng, H., Edwards, R.L., He, Y., Kong, X., An, Z., Wu, J., Kelly, M.J., Dykoski, C.A., Li, X., 2005. The Holocene Asian monsoon: links to solar changes and North Atlantic climate. Science 308, 854–857.
Wang, C., Li, X., Lai, Z., Tan, X., Pang, S., Yang, W., 2009. Seasonal variations of *Aulacoseira granulata* population abundance in the Pearl River Estuary. Estuar. Coast. Shelf Sci. 85, 585–592.
Wang, Z., Zhuang, C., Saito, Y., Chen, J., Zhan, Q., Wang, X., 2012. Early mid-Holocene sea-level change and coastal environmental response on the southern Yangtze delta plain, China: implications for the rise of Neolithic culture. Quat. Sci. Rev. 35, 51–62.
Wang, Z., Zhan, Q., Long, H., Saito, Y., Gao, X., Wu, X., Li, L., Zhao, Y., 2013. Early to mid-Holocene rapid sea-level rise and coastal response on the southern Yangtze delta plain, China. J. Quat. Sci. 28, 659–672.
Wang, Z., Ryves, D.V., Lei, S., Nian, X., Lv, Y., Tang, L., Wang, L., Wang, J., Chen, J., 2018. Middle Holocene marine flooding and human response in the south Yangtze coastal plain, East China. Quat. Sci. Rev (accepted).
van der Werff, A., Huls, H., 1976. Reprinted. In: Diatomeënflora van Nederland. Koeltz Science Publishers, Koenigstein (1957–1974) (1976).
Wilson, G.P., Lamb, A.L., Leng, M.J., Gonzalez, S., Huddart, D., 2005. $\delta^{13}C$ and C/N as potential coastal palaeoenvironmental indicators in the Mersey Estuary, UK. Quat. Sci. Rev. 24, 2015–2029.
Witkowski, A., Ichtiologii, D.R., Lange-Bertalot, H., Metzeltin, D., 2000. Diatom Flora of Marine Coasts I. A.R.G. Gantner Verlag K.G.
Xu, P., 2015. Research on the Archaeological Cultures of Neolithic Age in Ningzhen Area and Huantaihu Area. Jilin University, China (PhD Thesis, in Chinese, with English abstract).
Yan, Q., Huang, S., 1987. Evolution of Holocene sedimentary environment in the Hangzhou-Jiaxing-Huzhou Plain. Acta Geograph. Sin. 42, 1–15 (in Chinese, with English abstract).
Yang, S., Tang, M., Yim, W.W.S., Zong, Y., Huang, G., Switzer, A.D., Saito, Y., 2011. Burial of organic carbon in Holocene sediments of the Zhujiang (Pearl River) and Changjiang (Yangtze River) estuaries. Mar. Chem. 123, 1–10.
Yoneda, M., Uno, H., Shibata, Y., Suzuki, R., Kumamoto, Y., Yoshida, K., Sasaki, T., Suzuki, A., Kawahata, H., 2007. Radiocarbon marine reservoir ages in the western Pacific estimated by pre-bomb molluscan shells. Nucl. Inst. Methods Phys. Res. B 259, 432–437.
Yu, S., Zhu, C., Song, J., Qu, W., 2000. Role of climate in the rise and fall of Neolithic cultures on the Yangtze delta. Boreas 29, 157–165.
Zeng, L., Lesch, S.M., Grieve, C.M., 2003. Rice growth and yield respond to changes in water depth and salinity stress. Agric. Water Manag. 59, 67–75.
Zhang, J., Wu, Y., Jennerjahn, T.C., Ittekkot, V., He, Q., 2007. Distribution of organic matter in the Changjiang (Yangtze River) Estuary and their stable carbon and nitrogen isotopic ratios: implications for source discrimination and sedimentary dynamics. Mar. Chem. 106, 111–126.
Zhang, X., Huang, D., Deng, H., Snape, C., Meredith, W., Zhao, Y., Du, Y., Chen, X., Sun, Y., 2015. Radiocarbon dating of charcoal from the Bianjiashan site in Hangzhou: new evidence for the lower age limit of the Liangzhu Culture. Quat. Geochronol. 30 (Part A), 9–17.
Zheng, C.G., 2002. Environmental Archaeology on the Temporal-spatial Distribution of CULTURES sites in Taihu Lake Area During 7 ka BP – 4 ka BP. Nanjing University, China (PhD Thesis, in Chinese, with English abstract).
Zheng, Y., Sun, G., Chen, X., 2012. Response of rice cultivation to fluctuating sea level during the mid-Holocene. Chin. Sci. Bull. 57, 370–378.
Zheng, Y.F., Chen, X.G., Ding, P., 2014. Studies on the archaeological paddy fields at Maoshan site in Zhejiang. Quat. Sci. 34, 85–96.
Zhou, H., Zheng, X., 2000. The impact of environmental changes on the development of prehistoric civilization: the decline of the ancient Liang zhu culture in the Southern Plain of Yangtze River Delta. J. East China Norm. Univ. Nat. Sci. 4, 71–77 (in Chinese, with English abstract).
Zhu, N., 2006. Impacts of the rice farming on cultural development in the Taihu and Hangzhou Bay area. In: Museum, Shanghai (Ed.), Symposium on the Civilization Course of the Lower Reach Region of the Yangzte Rvier. Shanghai Book/Paint publishers, Shanghai, pp. 69–88 (in Chinese).

Zhuang, Y., Ding, P., French, C., 2014. Water management and agricultural intensification of rice farming at the late-Neolithic site of Maoshan, Lower Yangtze River, China. The Holocene 24, 531–545.
Zong, Y.Q., 2004. Mid-Holocene sea-level highstand along the southeast coast of China. Quat. Int. 117, 55–67.
Zong, Y., Chen, Z., Innes, J.B., Chen, C., Wang, Z., Wang, H., 2007. Fire and flood management of coastal swamp enabled first rice paddy cultivation in east China. Nature 449, 459–462.
Zong, Y.Q., Innes, J.B., Wang, Z.H., Chen, Z.Y., 2011. Mid-Holocene coastal hydrology and salinity changes in the east Taihu area of the lower Yangtze wetlands, China. Quat. Res. 76, 69–82.
Zong, Y., Wang, Z., Innes, J., Chen, Z., 2012a. Holocene environmental change and Neolithic rice agriculture in the lower Yangtze region of China: a review. The Holocene 22, 623–635.
Zong, Y., Innes, J.B., Wang, Z., Chen, Z., 2012b. Environmental change and Neolithic settlement movement in the lower Yangtze wetlands of China. The Holocene 22, 659–673.
Zuo, X., Lu, H., Jiang, L., Zhang, J., Yang, X., Huan, X., He, K., Wang, C., Wu, N., 2017. Dating rice remains through phytolith carbon-14 study reveals domestication at the beginning of the Holocene. Proc. Natl. Acad. Sci. U. S. A. 114, 6486.